

# Self-Isomerized–Cyclometalated Rhodium NHC Complexes as Active Catalysts in the Hydrosilylation of Internal Alkynes

Estefan van Vuuren, Frederick P. Malan, Werner Cordier, Margo Nell, and Marilé Landman\*

Corresponding Author

Marilé Landman – Department of Chemistry, University of Pretoria, Pretoria, South Africa 0002; orcid.org/0000-0003-4882-1142; Email: marile.landman@up.ac.za

Authors

Estefan van Vuuren – Department of Chemistry, University of Pretoria, Pretoria, South Africa 0002

Frederick P. Malan – Department of Chemistry, University of Pretoria, Pretoria, South Africa 0002

Werner Cordier – Department of Pharmacology, University of Pretoria, Pretoria, South Africa 0007

Margo Nell – Department of Pharmacology, University of Pretoria, Pretoria, South Africa 0007

## ABSTRACT

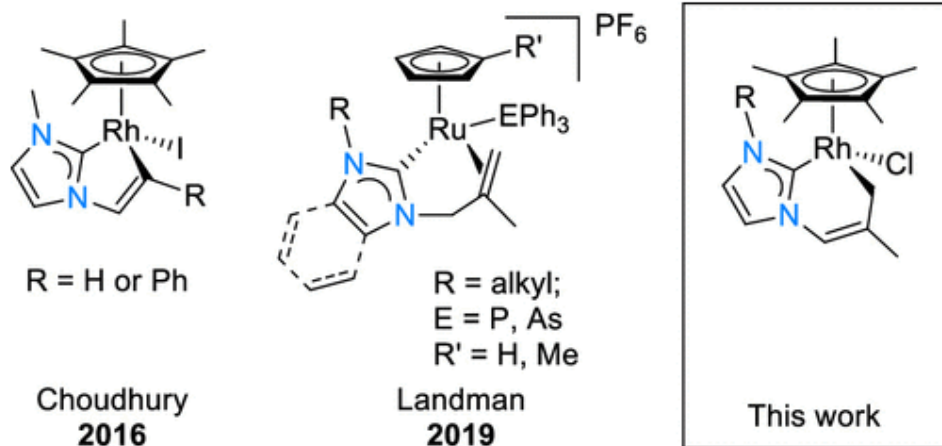
A range of unique Rh-based bidentate NHC complexes that are formed in a base-free tandem isomerization/cyclometalation process were synthesized (**1–4**) from a range of imidazolium salts with an *N*-alkenyl tether. Cyclometalation occurred with complex **1**, leading to an unprecedented complex, which is the first and only example in the literature of a nonaromatic C(sp<sup>2</sup>)–H activation leading to a C(sp<sup>3</sup>)–Rh cyclometalated product with a concomitant intramolecular/isomerization process. Dealkylation of the *N*-alkenyl substituent occurred to form byproducts that showed metal N-coordination (**1b** and **2b**). These byproducts, **1b** and **2b**, were further reacted with the anion exchange reagent NH<sub>4</sub>PF<sub>6</sub> to form the dimeric complexes **1bd** and **2bd**. All of the complexes were applied as precatalysts in the hydrosilylation of internal alkynes with excellent performance (conversions of 66–100%) after only 1 h at 80 °C without the use of an additive. Anticancer studies showed that complexes presented half-maximum inhibitory concentrations ranging from 3.71 to 25.85 μM. Depending on the cell line, complex **4** was the most cytotoxic complex, especially in the BT-20 triple-negative breast carcinoma, MCF-12A nontumorigenic mammary gland cell, MDA-MB-231 triple-negative breast carcinoma, and MCF-7/TAMR-1 tamoxifen-resistant subtype of the MCF-7 estrogen- and progesterone-positive luminal breast carcinoma cell lines.



## INTRODUCTION

Transition-metal complexes containing N-heterocyclic carbenes (NHCs) have been powerful tools in catalysis for the past 20 years, (1–4) with a wide variety of applications illustrating the general versatility of the metal NHC complexes. Even though rhodium is currently the most expensive member of the group IX transition metals, it is one of the most studied due to its high activity and stability. (5) Of the group IX metals, rhodium has proven to be the most active for C–H activation (6–13) in addition to being active for C–O, (14–16) C–C, (17) and C–N (18,19) activation reactions. (5,20) This was also observed in the work we describe herein, where a tandem isomerization/cyclometalation occurred via C–H bond activation of the *N*-tethered  $\beta$ -methyl allyl group on the NHC ligand. Inspired by these results, we decided to apply these complexes to one of the lesser studied hydrogenation reactions: namely, the hydrosilylation of internal alkynes. Hydrosilylation is considered as one of the most significant Si–C bond formation reactions in organosilicon chemistry due to its high atom economy and versatility to provide access to a plethora of functionalized silanes, important building blocks for organic molecules. (21,22) Rhodium complexes have previously been applied as highly active catalysts in these hydrosilylation processes; (21–24) however, the hydrosilylation of internal alkynes generally yields  $\beta$ -(*E*),  $\beta$ -(*Z*),  $\alpha$ -(*E*), and  $\alpha$ -(*Z*) isomers. Therefore, a regio- and stereoselective synthesis is desired, and in this study a range of rhodium-based NHC complexes have been developed for this application.

The rhodium complexes in this study were initially synthesized as analogues of previously studied ruthenium NHC complexes, (25,26) whereby the alkene-functionalized NHCs bonded in a bidentate fashion through C2 of the imidazolylidene ring and in a  $\eta^2$  fashion through the alkene tether (Landman, Figure 1).



**Figure 1.** Cyclometalation and isomerization of Rh-based NHC complexes.

In contrast to what was observed with these ruthenium complexes, a tandem cyclometalation with subsequent isomerization of the alkene bond occurred to form the bidentate rhodium complexes. This cyclometalated tether of the NHC ligand could confer extra activity through hemilability. (27) Dissociation of the cyclometalated arm from the metal center as a corresponding alkene allows for reversible substrate coordination, followed by rapid recoordination of the alkyl group via isomerization to stabilize the metal complex. Previously, a group led by Choudhury (10) synthesized cyclometalated Rh-NHC complexes (Choudhury, Figure 1), where cyclometalation was effected through a vinyl carbon in the

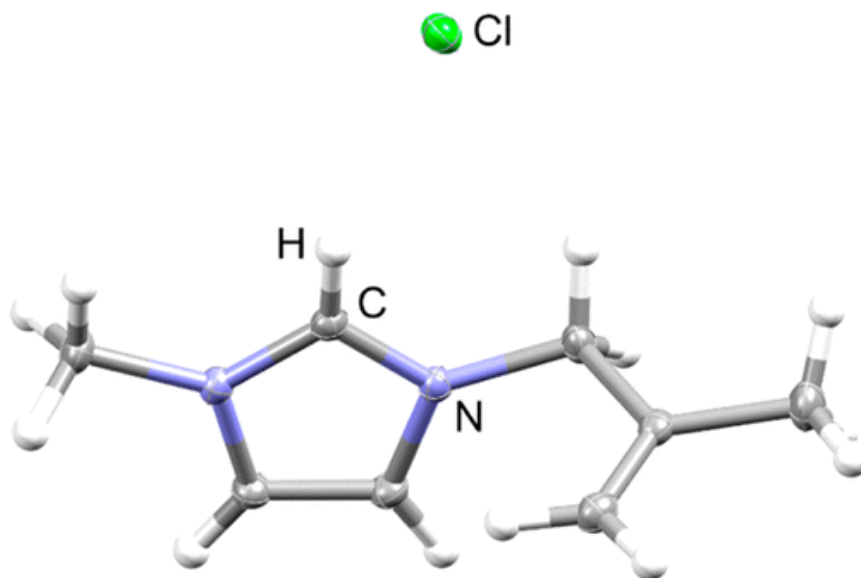
absence of functionality for isomerization, unlike in our work. Choudhury et al. (10) tested the reversibility of the C–H activation reaction by performing a H/D exchange experiment monitored by  $^1\text{H}$  NMR spectroscopy. They observed incorporation of deuterium into the styryl C–H bond, which suggested a high degree of reversibility for the activation of that bond, indicating that their complex confers hemilability. The cyclometalated complexes reported here (1–4) are the first and only examples in the literature, to our knowledge, of a nonaromatic  $\text{C}(\text{sp}^2)\text{--H}$  activation leading to a  $\text{C}(\text{sp}^3)\text{--Rh}$  cyclometalated product with a concomitant intramolecular/isomerization process. Complexes featuring C,C-chelating ligands of NHCs with a coordinated  $\text{C}(\text{sp}^3)$  remain rare, where selected examples of C–H activation of alkylnitrile (28) and phosphonium ylides (29,30) have been reported previously.

Herein we report the synthesis and characterization of eight novel rhodium(III) complexes, the evaluation of the catalytic activity of the complexes in the hydrosilylation of internal alkenes, and their cytotoxicity toward selected cancerous and noncancerous cell lines.

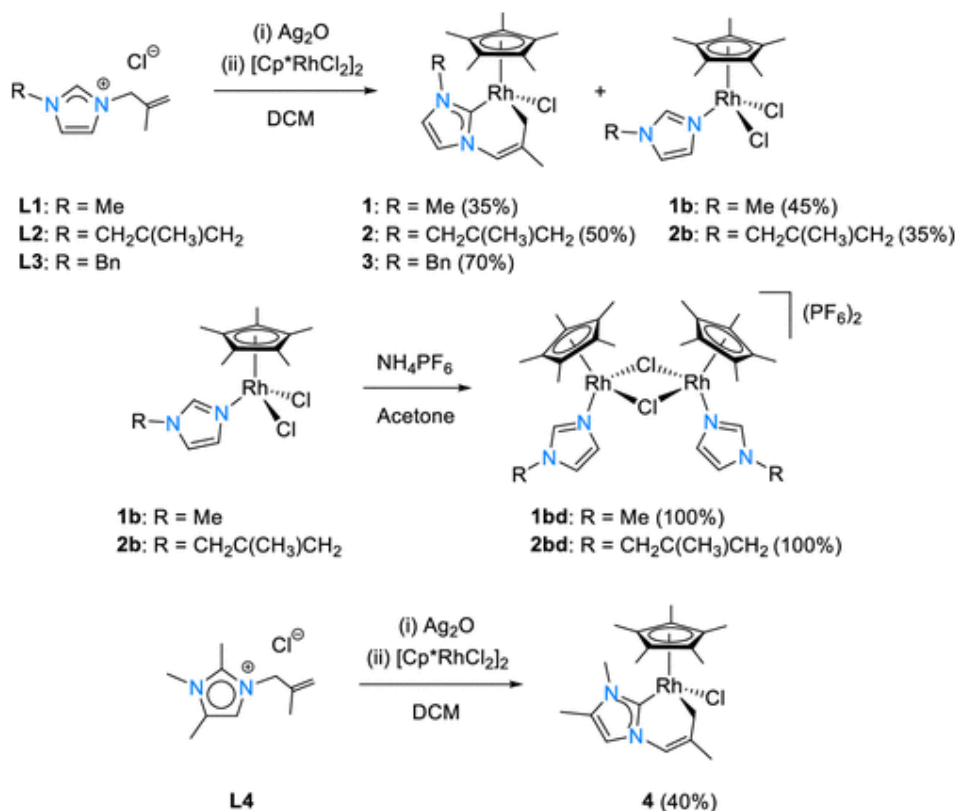
## RESULTS AND DISCUSSION

### Synthesis of the NHC Preligands

The NHC ligand precursors were synthesized by following a previously reported method. (25,26) The corresponding *N*-functionalized imidazoles were reacted with 3-chloro-2-methyl-1-propene in  $\text{CH}_3\text{CN}$  under reflux conditions, affording the corresponding alkene-tethered imidazolium chloride salts in good yields (**L1**, 94%; **L2**, 88%; **L3**, 91%; **L4**, 53%). (25,26) Washing of the salts with  $\text{Et}_2\text{O}$  or hexane removed any unreacted alkyl halide reagent to afford hygroscopic white to yellow compounds that varied in physical appearance (**L1**, **L2**, and **L4** as microcrystalline solids and **L3** as a yellow oil). Single crystals of **L1** suitable for single-crystal X-ray diffraction (SCXRD) were obtained by slow diffusion of a saturated  $\text{CH}_3\text{CN}/\text{Et}_2\text{O}$  (1/1) solution (Figure 2). Characterization by means of  $^1\text{H}$  and  $^{13}\text{C}$  NMR spectroscopy corresponds to previously reported literature data. (25,26)



**Figure 2.** Crystallographic representation of **L1** with thermal ellipsoids drawn at 50% probability. One  $\text{H}_2\text{O}$  molecule (solvent of crystallization) has been omitted for clarity.



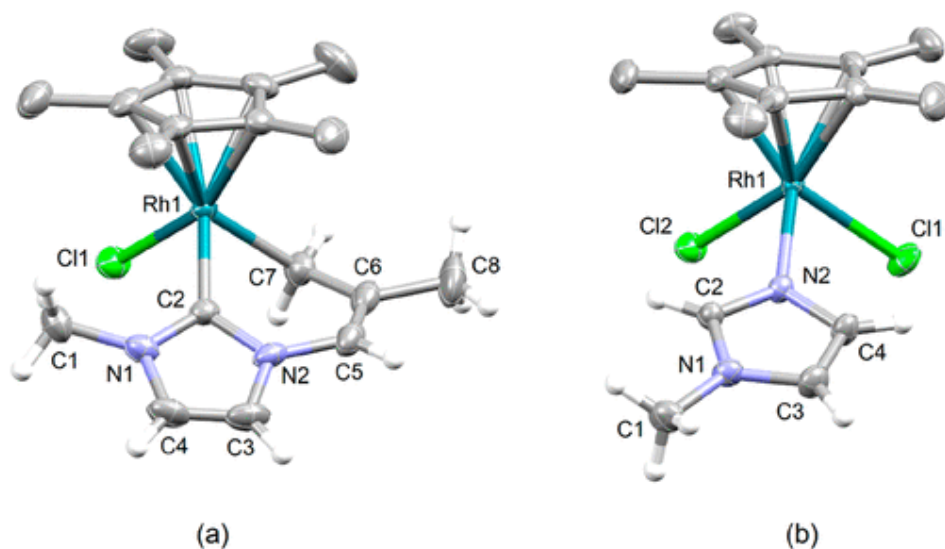
**Scheme 1.** General Scheme for the Synthesis of Rh(III) Complexes **1–4**, **1b**, **2b**, **1bd**, and **2bd**

### Synthesis of the Rhodium Complexes **1–4**, **1b**, **2b**, **1bd**, and **2bd**

Rhodium NHC complexes were synthesized by using the well-known transmetalation method with Ag<sub>2</sub>O (Scheme 1). The ligand precursor (**L1**) was added to excess Ag<sub>2</sub>O in CH<sub>2</sub>Cl<sub>2</sub> and the mixture stirred at 30 °C for 1 h to form the silver bis(carbene) intermediate. Preliminary reactions of the imidazolium salt with Ag<sub>2</sub>O revealed full conversion within 1 h, as evidenced by <sup>1</sup>H NMR spectroscopy: i.e., the complete disappearance of the acidic proton on the C2 position, with all of the remaining signals corresponding to the formation of a single silver carbene species (Figure S21 in the Supporting Information). Without isolation of the silver carbene, [Cp\*RhCl<sub>2</sub>]<sub>2</sub> was added to yield a dark red solution. Purification by means of column chromatography afforded the desired product as a yellow compound (**1**) in addition to a light red byproduct (**1b**). Complex **1** was recovered with a relatively low yield (35%) due to byproduct formation (**1b**, 45%). Initially it was suspected that the formation of the byproduct took place during the transmetalation step with Ag<sub>2</sub>O due to previously observed dealkylation of abnormal carbenes. (25,31,32) Therefore, the Ag-NHC formation step was shortened (from an initial 12 h to 1 h). The addition of an Ag carbene intermediate to the rhodium precursor complex hence leads to a possible rhodium-catalyzed *N*-dealkylation (33) of the imidazolylidene ligand. This occurs during the carbene transfer step to form the *N*-coordinated Rh byproduct complex as the major product. To further probe whether the *N*-dealkylation occurs via the Ag intermediate or by the Rh metal reagent, a standard direct metalation of **L1** to Rh with KO<sup>t</sup>Bu was attempted. Subsequently the same outcome was achieved: a crude <sup>1</sup>H NMR spectrum revealed the formation of **1** (30%), **1b** (50%), and

[Cp\*RhCl<sub>2</sub>]<sub>2</sub> (20%), as well as additional unidentified products, thus supporting possible rhodium-catalyzed *N*-dealkylation. Overall, the silver transmetalation strategy provided the best yield for **1** and was therefore used as the standard method of synthesis for the carbene formation reactions.

Spectroscopic evidence of NHC coordination in **1** was observed in the <sup>1</sup>H NMR spectrum, with the disappearance of the C2–H signal at 9.40 ppm along with the appearance of the carbene signal in the <sup>13</sup>C NMR spectrum between 175.2 and 175.8 ppm. A confirmation of cyclometalation was shown in the <sup>1</sup>H NMR spectrum, where a pair of doublets was observed at 1.95 (dd, *J* = 10.3, 3.5 Hz, 1H) and 3.41 ppm (d, *J* = 10.2 Hz, 1H), respectively, correlating with similar signals observed in the literature. (34) These peaks indicate coupling between the two unique geminal hydrogens located on the cyclometalated carbon, as well as with the NMR-active rhodium center. Additional 2D HSQC NMR data show the coupling between the <sup>1</sup>H and <sup>13</sup>C nuclei of the relevant hydrogen and carbon atoms of the σ-alkyl-tethered NHC moiety ligated to the rhodium center (Figure S3 in the Supporting Information). The isomerization of the alkene bond in **1** was confirmed by a far-downfield peak at 6.17 (s, 1H) ppm, suggesting a vinylic hydrogen. Other minor changes in the <sup>1</sup>H NMR spectrum of **1** (in comparison to that of **L1**) included the upfield shift of the imidazolylidene backbone protons (6.92 and 6.96 ppm in **1** vs 7.51 and 7.78 ppm in **L1**), as well as the slight downfield shift of the signal corresponding to the methyl group of the β-methylpropene tether in **1** (1.94 ppm in **1** vs 1.61 ppm in **L1**). The carbene carbon signal in the <sup>13</sup>C NMR spectrum appeared at 175.43 ppm as a doublet (*J*<sub>C–Rh</sub> = 58.7 Hz), whereas the signal of the cyclometalated carbon appeared at 21.0 ppm as a doublet (*J*<sub>C–Rh</sub> = 23.3 Hz). Both resonances are comparable to literature values of related complexes. (35) The byproduct **1b** was formed via probable Rh-mediated dealkylation of the *N*-substituted β-methylpropene group on the NHC ligand with subsequent coordination to the Rh center through this nitrogen atom of the imidazole ring. This dealkylation in **1b** was confirmed by its <sup>1</sup>H NMR spectrum in the disappearance of the allyl proton peaks as well as the appearance of the downfield C2–H proton signal at 7.86 ppm. The two backbone protons of the imidazole ring appeared at 6.88 and 7.13 ppm. Air-stable yellow-orange crystals of **1** as well as red crystals of **1b**, suitable for SCXRD, were grown from DCM/hexane mixtures, which allowed for confirmation of the molecular structures of **1** and **1b** (Figure 3), respectively. The structures of both half-sandwich Rh(III) complexes **1** and **1b** assumed a typical three-legged piano-stool geometry. Selected bond lengths and angles are summarized in the caption of Figure 3. For additional crystallographic parameters and information, see Tables S1 and S3 in the Supporting Information.



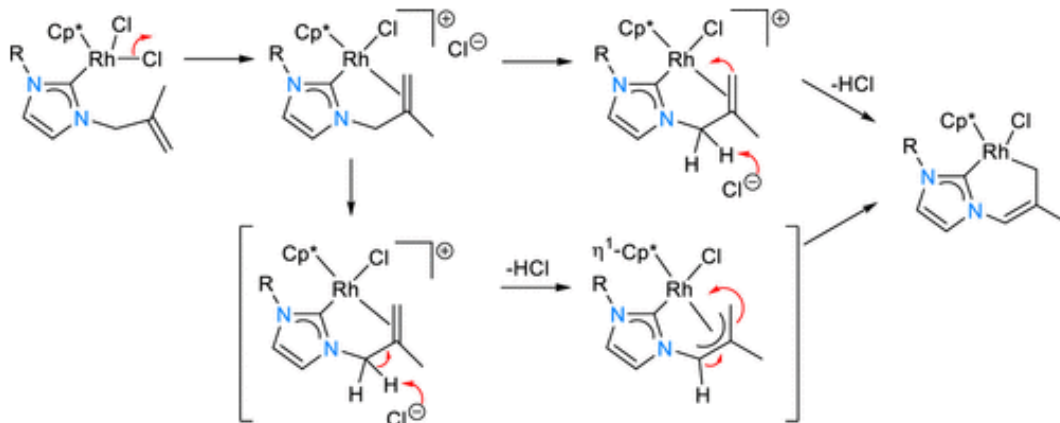
**Figure 3.** Crystallographic representations of (a) **1** and (b) **1b** with thermal ellipsoids drawn at 50% probability. Hydrogen atoms of the Cp\* groups in both structures have been omitted for clarity. One H<sub>2</sub>O molecule (solvent of crystallization) in the structure of **1b** is omitted for clarity. Important bond lengths (Å) and angles (deg): **1**, Rh(1)–Cl(1) = 2.4219(14), Rh(1)–C(2) = 1.990(5), Rh(1)–C(7) = 2.095(6), C(5)–C(6) = 1.302(8), C(6)–C(7) = 1.476(8), Rh(1)–C(7)–C(6) = 115.0(4), C(5)–C(6)–C(7) = 121.8(6), C(2)–Rh(1)–C(7) = 81.6(2); **1b**, Rh(1)–Cl(1) = 2.4401(9), Rh(1)–N(2) = 2.107(3), Cl(1)–Rh(1)–Cl(2) = 89.96(4), Cl(1)–Rh(1)–N(2) = 88.32(8).

The Rh–C<sub>NHC</sub> bond length in **1** was found to be 1.990(5) Å, which is shorter than similar bonds found in the literature (2.008–2.081 Å). (36–38) As expected, the Rh–C<sub>cyclometalated</sub> bond in **1** (2.095(6) Å) was longer than the Rh–C<sub>carbene</sub> bond; the bond length, however, compared well to Rh–C<sub>cyclometalated</sub> bonds in similar complexes found in the literature (2.032–2.123 Å). (37) The isomerization in **1** is reflected in the shorter C5–C6 bond (double-bond character) of 1.302(8) Å (1.5042(18) Å in **L1**, single-bond character), as well as the longer C6–C7 bond (single bond) of 1.476(8) Å (1.3190(19) Å in **L1**, double bond). The six-membered metallacycle in **1** is pseudoplanar to the NHC ligand plane (torsion angles C2–N2–C5–C6 = –20.4(9)° and N2–C5–C6–C7 = –3.24(10)°).

The NHC ligand in **1** binds in a chelating fashion with a bite angle of 81.6(2)°, slightly larger than what was reported in related examples in the literature (79.0–81.06°). (37) The Rh(1)–N(2) distance in **1b** was found to be 2.107(3) Å, similar to Rh–N bond lengths found in the literature (2.085(5)–2.136(3) Å). (39)

An attempt was made to observe the formation of an Rh–H species, an intermediate proposed in the literature for cyclometalation mechanisms, (40) through sampling of the reaction mixture during synthesis of the NHC complex. However, no characteristic hydride peak was observed, which does not preclude this as a reaction route but may suggest that this intermediate is merely short lived. In addition, a chloride deprotonation method was proposed (Scheme 2) as an alternative mechanism, proceeding through an allyl-coordinating intermediate. The NMR sample that was taken during the synthesis of the NHC complex did show an HCl peak at 8.04 ppm (broad singlet; see Figure S22 in the Supporting Information). HCl is formed as a byproduct in both proposed mechanisms.

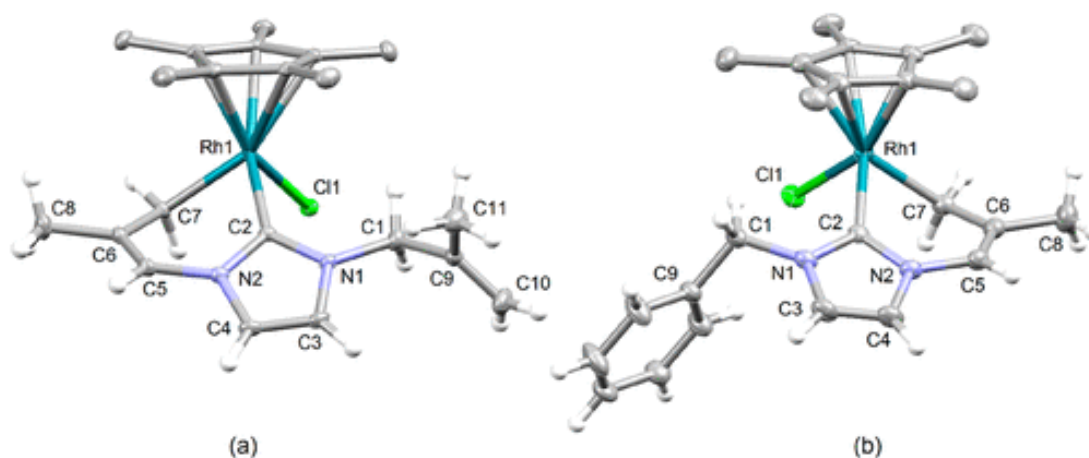




**Scheme 2.** Proposed Mechanism for Isomerization-Cyclometalation via an Allyl-Coordinating Rh(III) NHC Complex

In the related silver transmetalation reaction of  $[\text{Cp}^*\text{RhCl}_2]_2$  with **L2**, an imidazolium chloride salt containing two *N*-alkenyl tether groups, a similar outcome was achieved: a yellow complex, **2** (yield 48%), and the red byproduct **2b** were again isolated from this reaction. Proof of cyclometalation in **2** was once again confirmed by the  $^1\text{H}$  NMR spectrum, where a vinylic proton signal was observed far downfield (s, 6.18 ppm, 1H) while the splitting of the hydrogens on the cyclometalated carbon at  $\delta$  2.00–1.97 (m, 1H) and 3.39–3.43 ppm (m, 1H) was seen as a doublet. Supporting 2D HSQC NMR data furthermore agree with the structure assigned to **2** (Figure S11 in the Supporting Information).  $^1\text{H}$  NMR signals corresponding to the free alkenyl tether appeared at 1.81 (methyl group), 4.83, 5.25 (methylene protons), and 4.96, 5.06 ppm (terminal alkene), which does not suggest that any alkene isomerization has taken place in the free alkenyl arm. The  $^1\text{H}$  NMR spectrum of **2b** revealed signals pertaining to a free *N*-alkenyl group as well: 1.65 (methyl group), 4.84, 4.77 (terminal alkene protons), and 4.40 ppm (methylene protons). The imidazole ring backbone protons appeared at 6.86 and 6.95 ppm, with its downfield-shifted C2–H signal being found at 7.91 ppm, an overall good comparison with the corresponding  $^1\text{H}$  NMR signals of **1b**. As part of a further investigation into the tendency of the rhodium center to cyclometalate NHC-based ligands in forming six-membered metallacycles, **L3** was employed, which contained both an *N*-alkenyl tether and an *N*-benzyl tether. Either of these functional groups are able to cyclometalate to Rh to form six-membered rhodacycles. (41) In contrast to previous observations (co-formation of **1** and **1b**, as well as of **2** and **2b**), the synthesis of **3** did not yield any side products and in fact was isolated with the highest yield of all the complexes (70% yield). Exclusive cyclometalation–isomerization of the alkenyl arm was deduced from the  $^1\text{H}$  NMR spectrum, whereby the set of doublet signals of the protons on the cyclometalated carbon was observed at 2.05 (ddd,  $J = 10.3, 3.6, 1.3$ , 1H) and 3.49 ppm (dt,  $J = 10.5, 3.2$  Hz, 1H). Peaks corresponding to a free benzyl tether was observed at 5.25, 6.11 (methylene protons) and 7.34–7.53 ppm (phenyl protons). Signals pertaining to the inequivalent imidazolylidene backbone protons appeared at 6.73 and 6.91 ppm, which is in good correlation with related signals in **1** and **2**. The carbene carbon signals in the  $^{13}\text{C}$  NMR spectra of **2** and **3** appeared slightly downfield at 176.0 ppm as a doublet ( $J_{\text{C-Rh}} = 59.2$  Hz) and at 175.9 ppm as a doublet ( $J_{\text{C-Rh}} = 58.8$  Hz) in comparison to related signals in **1** (175.4 ppm). The  $^{13}\text{C}$  NMR signals of the cyclometalated carbon atoms in **2** and **3** appeared at 21.2 (d,  $J_{\text{C-Rh}} = 23.2$  Hz) and 21.3 ppm (d,  $J_{\text{C-Rh}} = 23.1$  Hz), which compare well with the corresponding signal in the  $^{13}\text{C}$  NMR spectrum of **1**.

Orange-yellow crystals of **2** and yellow crystals of **3** suitable for SCXRD analysis were grown from saturated CH<sub>2</sub>Cl<sub>2</sub> solutions. The molecular structures of **2** and **3** each reveal a six-coordinate three-legged piano-stool geometry around the central Rh atom, similar to the case for **1**. Selected bond lengths and angles are summarized in the caption of Figure 4. Additional crystallographic parameters and information are contained in Table S2 in the Supporting Information. The Rh–C<sub>NHC</sub> bonds of **2** and **3** were found to be longer than that of **1** at 2.0045(16) Å (**2**) and 2.010(4) Å (**3**), comparable to those found in the literature for similar complexes (2.010–2.081 Å). (36–38) The cyclometalated NHC ligands in **2** and **3** bonded to the rhodium center with bite angles of 82.69(7) (**2**) and 82.70(16)° (**3**), which in both cases are larger than that of **1**, and deviated further from the values reported in the literature of ca. 79.0–81.06°. (37) It can be concluded from our observations that cyclometalation through the allyl arm is preferred; this could be further explored in the future by functionalizing the NHC ligand framework with additional groups that are susceptible to cyclometalation: for example, mesityl, (35) phenyl, (42) pyridyl, (43) and bis(carbene) (44) groups. As with **1**, the six-membered metallacycles in **2** and **3** are both pseudoplanar to the NHC ligand plane (torsion angles C2–N2–C5–C6 = 23.8(3)° (**2**), –21.5(7)° (**3**) and N2–C5–C6–C7 = 3.55(5)° (**2**), –2.80(4)° (**3**)), with the rhodium center pointing upward (torsion angles Rh1–C2–N2–C5 = 0.7(2)° (**2**), –6.1(6)° (**3**) and Rh1–C7–C6–C5 = –48.4(2)° (**2**), 47.0(5)° (**3**)).

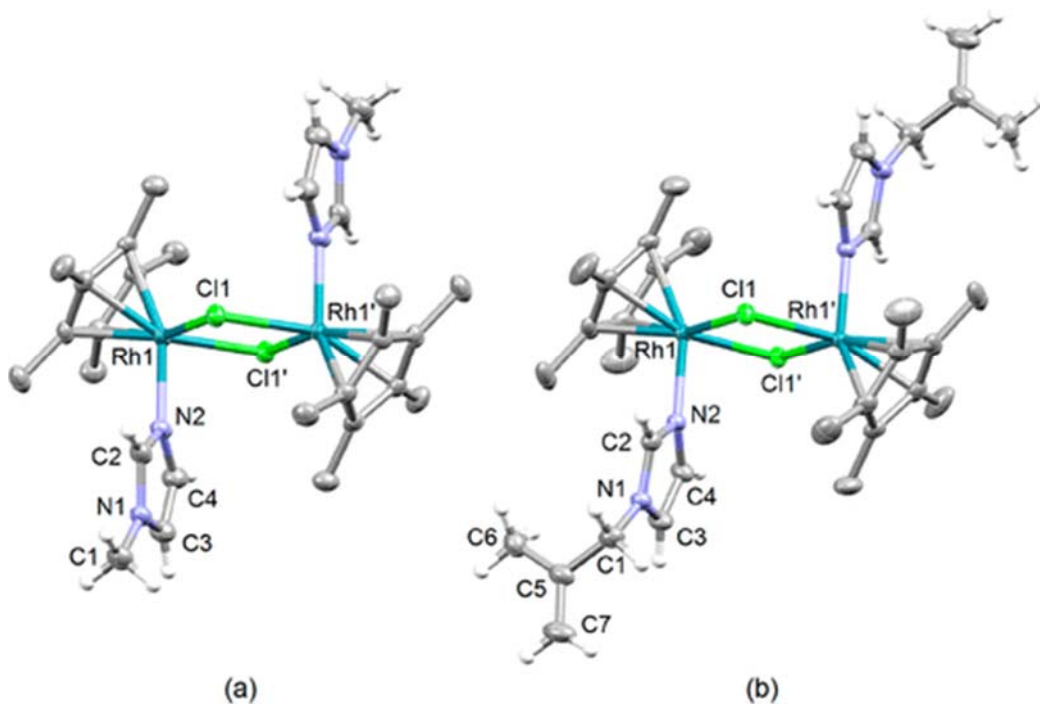


**Figure 4.** Crystallographic representation of cyclometalated complexes (a) **2** and (b) **3** with thermal ellipsoids drawn at 50% probability. Hydrogen atoms of the Cp\* groups in both structures have been omitted for clarity. Important bond lengths (Å) and angles (deg): **2**, Rh(1)–Cl(1) = 2.4260(4), Rh(1)–C(2) = 2.0045(16), Rh(1)–C(7) = 2.0898(16), Rh(1)–C(7)–C(6) = 115.57(11), C(5)–C(6)–C(7) = 122.21(16), C(2)–Rh(1)–C(7) = 82.69(7); **3**, Rh(1)–Cl(1) = 2.4239(10), Rh(1)–C(2) = 2.010(4), Rh(1)–C(7) = 2.098(4), Rh(1)–C(7)–C(6) = 114.9(3), C(5)–C(6)–C(7) = 122.3(4), C(2)–Rh(1)–C(7) = 88.70(12).

In an attempt to improve the catalytic performance of **2b** (*vide infra*), it was reacted with NH<sub>4</sub>PF<sub>6</sub> in acetone, resulting in the formation of the dimeric complex **2bd**. The aim in the design of **2bd** was 2-fold: (i) in recent studies (25,26) the performance of cationic complexes showed higher reactivity in comparison to the corresponding neutral analogues and (ii) by using a dimeric catalyst, a vacant coordination site is readily created by cleavage of the complex with addition of the incoming substrate (in our case an alkyne). On the basis of the results in the formation of **2bd**, the reaction with NH<sub>4</sub>PF<sub>6</sub> in acetone was repeated for **1b** to form the complex **1bd**. The <sup>1</sup>H NMR spectra of each of these complexes appeared simplistic,



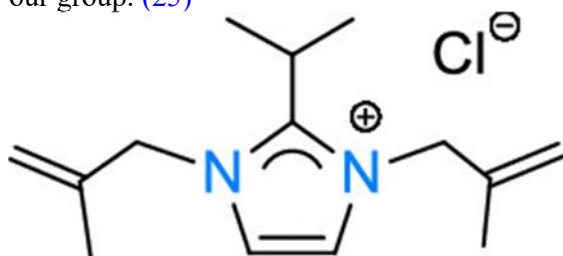
with signals corresponding to the Cp\* and imidazole ligands in a 1:1 ratio: complex **1bd** exhibited signals at 8.11 (C2–H of imidazole), 7.33, 7.34 (backbone protons of imidazole) and 1.63 and 1.76 ppm (Cp\*), whereas complex **2bd** displayed signals at 8.17 (C2–H of imidazole), 7.39, 7.33 (backbone protons of imidazole), and 1.66, 1.67 ppm (Cp\*). Additional signals related to the unique *N*-alkyl groups of each of the complexes correspond closely to those of the mononuclear derivatives **1b** and **2b**, respectively. Single crystals for both complexes **1bd** and **2bd**, suitable for SCXRD, were obtained from the slow evaporation of saturated acetone solutions. The molecular structures of **1bd** and **2bd** each reveal the typical six-coordinate geometry around each of the rhodium centers, similar to the structure of the mononuclear complex **1b**. Selected bond lengths and angles are summarized in the caption of Figure 5, while other crystallographic parameters and information are contained in Table S1 in the Supporting Information. Comparable bond lengths and angles have been observed among the structures of **1b**, **1bd**, and **2bd**. The synthetic versatility of **1bd** and **2bd** might render them interesting and easily accessible precursors to mononuclear Cp\*RhCl(L)(imidazole) complexes through simple, single bond-cleaving reactions with 2 equiv of a neutral L ligand.



**Figure 5.** Crystallographic representation of cyclometalated complexes (a) **1bd** and (b) **2bd** with thermal ellipsoids drawn at 50% probability. Hydrogen atoms of the Cp\* groups in both structures have been omitted for clarity. Important bond lengths (Å) and angles (deg): **1bd**, Rh(1)–Cl(1) = 2.4622(9), Rh(1)–N(2) = 2.099(3), Cl(1)–Rh(1)–Cl(2) = 83.90(3), Cl(1)–Rh(1)–N(2) = 88.66(10); **2bd**, Rh(1)–Cl(1) = 2.4430(10), Rh(1)–N(2) = 2.102(3), Cl(1)–Rh(1)–Cl(2) = 85.16(3), Cl(1)–Rh(1)–N(2) = 88.28(10).

As an interesting addition to the rhodium complex series, it was decided to investigate the mode of NHC coordination (normal vs abnormal) on the reaction outcome in light of the (side) reactions discussed above, as well as changes in the general stability and reactivity of the resultant Rh NHC complexes. Initially a different imidazolium salt (**L5**, Figure 6), with an isopropyl blocking group on C2 of the imidazole ring, was reacted with the Rh precursors; however, no isolable products were obtained, and therefore **L4** was used in the hope of

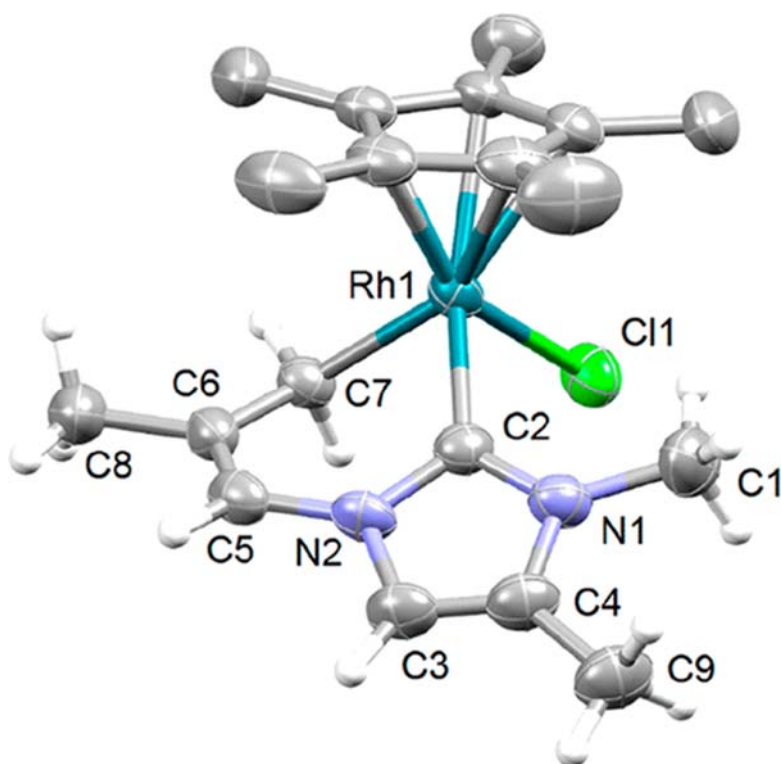
obtaining a mixture of normally bound and abnormally bound products as observed before by our group. (25)



## L5

**Figure 6.** Imidazolium salt with an isopropyl blocking group.

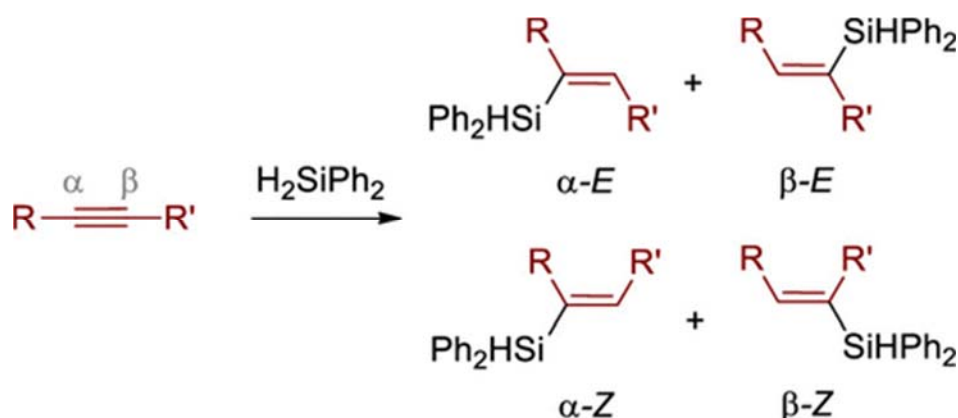
This reaction, unlike those with the NHC precursors leading to normal (C2-coordinated) NHC metal complexes, for formation of the abnormal (C4-coordinated) silver carbene complex from the reaction of imidazolium salt **L4** and Ag<sub>2</sub>O required an overnight reaction (>12 h). (25) Subsequent filtration, addition of [Cp\*RhCl<sub>2</sub>]<sub>2</sub>, and stirring for 18 h resulted in the formation of a dark red solution. Purification by column chromatography afforded the yellow main product **4** in a modest yield (30%) in addition to unreacted starting material. Interestingly, it was observed via <sup>1</sup>H NMR and <sup>13</sup>C NMR spectroscopy that complex **4** does not contain a methyl group on position C2, which means dealkylation occurred at the C2 position, resulting in the formation of a normal carbene bond rather than the expected abnormal carbene bond. This is in line with what has previously been observed by both our group (25) and others. (31,32,45,46) Cyclometalation is confirmed as before with a set of signals observed in the <sup>1</sup>H NMR spectrum at 3.44 (dd, *J* = 6.9, 3.3 Hz, 1H, Rh-CH<sub>2</sub>) and 1.99–2.03 ppm (m, 1H, Rh-CH<sub>2</sub>) for the protons of the cyclometalated carbon atom. Isomerization was also confirmed by the presence of the signal corresponding to a vinylic proton at 6.13 (s, 1H, NCH=C) ppm. The carbene carbon signal in the <sup>13</sup>C NMR spectrum of **4** appeared at 173.6 ppm (d, *J*<sub>C-Rh</sub> = 58.7 Hz), similar to that of complexes **1–3**, which confirms the normal coordination mode, since abnormal carbene signals show a distinct upfield shift from the normal carbene carbon signal. (25) The <sup>13</sup>C NMR signals of the cyclometalated carbon atom of **4** appeared at an expected position of 20.2 ppm (d, *J*<sub>C-Rh</sub> = 23.3 Hz). A crystal suitable for SCXRD spectroscopy was obtained from slow diffusion of a saturated DCM/hexane solution, allowing the molecular structure of **4** to be determined (Figure 7). The structural data of **4** are very similar to those of **1**, with the only difference being the addition of a methyl group on the backbone of the imidazole. This electron-donating group possibly conferred some additional electron density on the imidazolium ring, resulting in a relatively short Rh–C<sub>carbene</sub> bond (Rh1–C2 = 2.015(6) Å). The six-membered metallacycle in **4** is pseudoplanar to the NHC ligand plane (torsion angles C2–N2–C5–C6 = 18.0(10)° and N2–C5–C6–C7 = 3.6(10)°), with the rhodium center pointing upward, resembling a half-boat conformation (torsion angles Rh1–C2–N2–C5 = 8.7(9)° and Rh1–C7–C6–C5 = –45.1(8)°). The NHC ligand in **4** binds in a chelating fashion with a bite angle of 83.2(3)°.



**Figure 7.** Crystallographic representation of cyclometalated complex **4** with thermal ellipsoids drawn at 50% probability. Hydrogen atoms of the Cp\* groups and H<sub>2</sub>O molecule have been omitted for clarity. Important bond lengths (Å) and angles(deg): Rh(1)–Cl(1) = 2.4206(18), Rh(1)–C(2) = 2.015(6), Rh(1)–C(7) = 2.100(6), C(5)–C(6) = 1.311(10), Cl(1)–Rh(1)–C(2) = 92.69(19), Cl(1)–Rh(1)–C(7) = 89.31(19), C(2)–Rh(1)–C(7) = 83.2(3).

### Catalytic Hydrosilylation

Due to the known activity of Rh for the activation of C–H bonds, as observed in the formation of the Rh complexes described herein, we anticipated our complexes to be highly active toward the hydrosilylation of internal alkynes. Internal alkynes are generally considered to be fairly inert toward a variety of transformation reactions in comparison to their terminal alkyne counterparts, (47–49) and therefore a catalyst that can effectively and selectively hydrosilylate internal alkynes would be very useful. Previous studies on Rh-NHC catalysts with *N*-donor-functionalized ligands exhibited good activity (50) toward the hydrosilylation of terminal alkynes, where the majority of these catalysts, however, produced low selectivities. (51–53) The hydrosilylation of internal alkynes provides four possible products, the  $\alpha$ -(*E*),  $\alpha$ -(*Z*),  $\beta$ -(*E*), and  $\beta$ -(*Z*) alkene isomers (Scheme 3).



**Scheme 3.** General Reaction of Internal Alkyne with Diphenylsilane Yielding the Four Possible Isomers  $\alpha$ -(*E*),  $\alpha$ -(*Z*),  $\beta$ -(*E*), and  $\beta$ -(*Z*)

The catalytic activity of the synthesized rhodium complexes as precatalysts in the hydrosilylation reaction of internal alkynes was studied using an adjusted literature method. (22) Diphenylacetylene was used as the substrate and **2** as the precatalyst to determine the optimal conditions (Table 1). A catalyst screening was conducted under optimal conditions to determine the most active catalyst among the novel rhodium complexes. Coincidentally, complex **2** exhibited the highest activity and second highest selectivity in the conversion of diphenylacetylene to its respective *E* product. It was found that after 40 min **2** showed a conversion of 99% (Graph S1 in the Supporting Information), while after 60 min a full conversion of 100% was obtained. The reaction gave a TOF of 92.9 h<sup>-1</sup> after 10 min. On comparison of the activities of the N-Me (**1**) and N-Bn (**3**) catalysts with that of **2**, both **1** and **3** exhibited slightly lower activities (93% conversion, entries 8 and 9 versus entry 3), with comparable product selectivities. The reasons for this lowered activity are unclear at this stage, where steric arguments cannot be made, as both a less steric substituent (N-Me) and a bulkier substituent (N-Bn) gave rise to similar results. However, having an additional flexible alkenyl tether present in **2**, as opposed to **1** and **3**, might confer additional stability on the catalytic intermediates via rapid coordination and dissociation. This is also believed to be true in the cases of **1** and **2** (each exhibiting a bidentate NHC), as opposed to **1b** and **2b** (each featuring a monodentate N-bound imidazole ligand); additional stability to sensitive intermediates is provided via the metallacycle in **1** and **2**, which exhibited higher activities in comparison to **1b** and **2b**. Using **2** at 4 mol % catalyst loading, the conversion was found to be the highest (100%, entry 2), at the cost of selectivity (73% toward the *E* product). At lower catalyst concentrations the selectivity toward *E* increased to values as high as 84% when 1 mol % catalyst was used, associated with a marginal decrease in conversion (76%, entry 6). Expectedly, it can be noted that higher TOFs are observed at lower catalyst loadings; however, the decision to continue with 4 mol % loading as the optimal catalyst concentration was made to maximize conversion—especially for reactions where more inert substrates are employed. Higher temperatures (80 °C) seemed to favor the formation of the *E* isomer, while at a temperature of 50 °C the *Z* isomer was formed (entry 7). Similarly, shorter reaction times (1 h) promoted formation of the *E* isomer, while after a longer reaction time (>3 h), the *Z* isomer was dominant (entries 4 and 7). Addition of a base to **2b** in order to create a vacant coordination site on the metal resulted in 96% conversion (entry 12), improving the conversion without affecting the selectivity. An alternative method of creating a vacant coordination site was to employ **2bd** as a precatalyst, where cleavage of the complex with the substrate formed an active site *in situ*. The conversions were similar (entry 13 vs entry 12) but the selectivity for the *E* isomer increased to 90%.


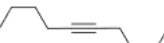
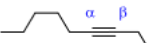
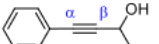
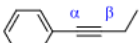
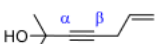
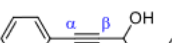

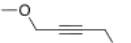
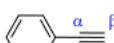

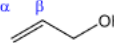
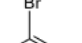
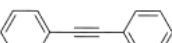
**Table 1.** Method Optimization and Catalyst Screening for Hydrosilylation of Diphenylacetylene<sup>a</sup>

entry	complex	catalyst loading (mol %)	temp (°C)	conversion (%)	yield (%)	selectivity (%)		TOF <sup>d</sup> (h <sup>-1</sup> )
						E	Z	
1			80	0				
2	<b>2</b>	8	80	100	70	75	25	12.6
3	<b>2</b>	4	80	100	73	74	26	25.2
4 <sup>b</sup>	<b>2</b>	4	RT	33	26	50	50	8.32
5	<b>2</b>	2	80	82	48	84	16	41.2
6	<b>2</b>	1	80	76	53	79	21	76.4
7 <sup>c</sup>	<b>2</b>	4	50	38	31	36	64	9.62
8	<b>1</b>	4	80	93	65	72	28	23.5
9	<b>1b</b>	4	80	72	50	72	28	18.1
10	<b>1bd</b>	4	80	85	51	65	35	21.4
11	<b>2b</b>	4	80	66	50	68	32	16.6
12 <sup>c</sup>	<b>2b</b>	4	80	96	43	67	32	24.2
13	<b>2bd</b>	4	80	92	46	90	10	23.2
14	<b>3</b>	4	80	93	76	77	23	23.3
15	<b>4</b>	4	80	94	55	58	42	23.7

<sup>a</sup>General conditions unless specified otherwise: PhC≡CPh (18 mg, 0.1 mmol), H<sub>2</sub>SiPh<sub>2</sub> (11 μL, 0.1 mmol), Rh precatalyst (4 mol %), anisole (10 μL, 0.11 mmol), C<sub>6</sub>D<sub>6</sub>, 80 °C, 1 h. <sup>b</sup>After 24 h 96% conversion (NMR yield of 77%) was observed with *E*:*Z* = 20%:80%. <sup>c</sup>After 3 h 86% conversion (NMR yield of 43%) was observed with *E*:*Z* = 32%:68%. <sup>d</sup>After 1 h. <sup>e</sup>Reaction done with the addition of 10 mol % of K<sub>2</sub>CO<sub>3</sub> as an additive.

In comparison to the catalysis of diphenylacetylene by Hollis et al., (22) their homobimetallic rhodium NHC complex (catalyst loading of 2–3.5 mol %) achieved 100% conversion after 2 h at 80 °C with a selectivity of 80% *E* and 20% *Z*, whereas our cyclometalated complex **2** had a conversion of 100% after only 1 h with slightly lower selectivity for the *E* isomer (entry 3). Young and co-workers (54) tested their PC<sub>carbene</sub>P pincer complex for the hydrosilylation of phenylacetylene among other alkynes. They conducted their reactions at room temperature with a reaction time of 24 h; however, they only achieved 35% conversion but with good *E* isomer selectivity (*E*:*Z* = 98:2), whereas our complex **2** had an almost quantitative conversion after 24 h at room temperature but high selectivity for the *Z* isomer (80%). Even at a catalyst loading of 1 mol %, **2** performed admirably with a conversion of 76% after only 1 h (selectivity of 79% *E* and 21% *Z*), in comparison to the triazolium-based Rh(I) complex of Álvarez and co-workers, (55) where they achieved higher conversion and selectivity (99% with 96% *E* vs 4% *Z*) after 1 h with a catalyst loading of 1 mol %.

**Table 2.** Substrate Screening Using **2** as a Precatalyst for the Hydrosilylation of Internal Alkynes<sup>a</sup>

Entry	Substrate	Conversion (%) <sup>b</sup>	Yield (%) <sup>b</sup>	Selectivity (%) <sup>c</sup>	
				<i>E</i>	<i>Z</i>
1		97	49	90	10
2		100	70	97	3
3 <sup>d</sup>		96	49	43 (22)	20 (15)
4		93	63	25 (25)	23 (27)
5		96	78	56 (36)	8 (-)
6		99	53	25 (23)	20 (32)
7		100	67	22 (21)	20 (37)
8		97	47	40(21)	27 (12)
9		83	83	72	28
10 <sup>e</sup>		75	50	39 (29)	32
11 <sup>e</sup>		95	33	57 (-)	43
12		95	94	n.a.	
13 <sup>f</sup>		95	87	n.a.	
14		100	62	74	26

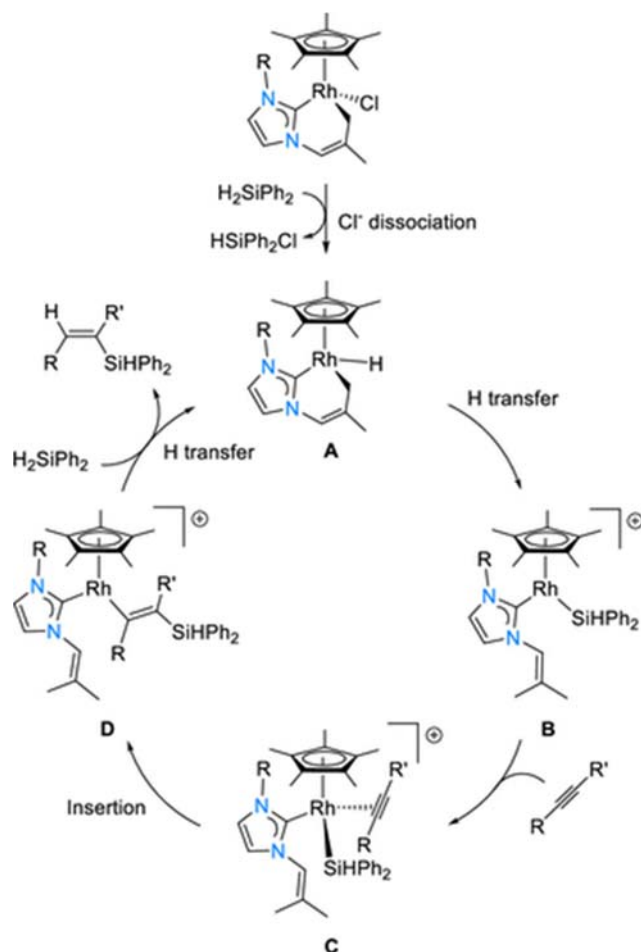
<sup>a</sup>General reaction conditions: alkyne (18 mg, 0.1 mmol), H<sub>2</sub>SiPh<sub>2</sub> (11  $\mu$ L, 0.1 mmol), Rh precatalyst (4 mol %), anisole (10  $\mu$ L, 0.11 mmol), C<sub>6</sub>D<sub>6</sub>, 80 °C, 1 h. <sup>b</sup>The conversion calculation (%) is based on the consumption of H<sub>2</sub>SiPh<sub>2</sub>, n.a. = not applicable. <sup>c</sup>For the asymmetric substrates the values given represent the selectivity for the  $\beta$  isomer, while the percentages in parentheses indicate selectivity for the  $\alpha$  product formed. <sup>d</sup>For all of the asymmetric alkyne substrates, the  $\alpha$ - and  $\beta$ -carbon atoms are indicated here. <sup>e</sup>For terminal alkynes only one  $\alpha$  product is formed, the percentage of which is indicated in parentheses. <sup>f</sup>Only one product formed: (3-bromobutyl)diphenylsilane.

Complex **2** was again employed as a precatalyst for the substrate screening study (Table 2), since it was found to be highly active for the range of substrates selected, with high conversions observed (75–100%), therefore suggesting a good functional group tolerance. Both symmetrical and asymmetrical alkynes were screened which included selected alcohol containing alkynes. The alcohol functional groups could coordinate to the metal center during catalysis, thereby reducing activity of the active catalyst as found by Hollis, (22) where in their study the substrates 1-hexyn-3-ol and 1-ethynyl-1-cyclohexanol required longer reaction times to give a final conversion of 100% for both after ~7 h (in comparison to 2 h with diphenylacetylene) using 2–3.5 mol % of Rh catalyst. This was not found to be the case in our study, however, where the alcohol-containing alkynes were nearly completely converted after only 1 h (93–100%). Interestingly, for the internal alkyne series, 1,4-dimethoxy-2-butyne (entry 9) was the least successfully converted (83%), which could not be ascribed to direct steric or electronic reasons in comparison to the other substrates such as diphenylacetylene, 1-phenyl-4-methyl-1-pentyn-3-ol, 2-methyl-6-hepten-3-yn-2-ol, and 1-



phenyl-1-hexyn-3-ol (entries 14, 4, 6, and 7, respectively), where high conversions (93–100%) and good yields (53–67%) were achieved. Expanding the substrate scope to include terminal alkynes and internal/terminal alkenes yielded similar results of high conversions (75–95%) and good yields (50–94%) except for the case of 1-hexyne, which had a yield of 33%. Hydrosilylation of terminal alkynes allows for the formation of three products: the  $\beta$ -(*E*),  $\beta$ -(*Z*), and  $\alpha$  products. In the case of terminal alkynes complex **2** was not as active (see entries 10 and 11, Table 2) in comparison to literature reports (conversions of 98–99% at lower temperatures for 20 min). (56) For the hydrosilylation of alkenes (see entries 12 and 13, Table 2), complex **2** performed comparably to the results (conversions of 95–97% at RT after 12 h) obtained by Huertos et al. (57) All of the substrates (entries 1–14) had similar TONs (20.4–25.2) due to the similarly high conversions obtained throughout the substrate scope.

The standard Chalk–Harrod mechanism of the group IX metal catalyzed hydrosilylation reaction of alkynes typically involves the formation of the  $M^{III}H(SiHR_2)$  or  $M^{III}H(SiR_3)$  species, depending on the organosilicon substrate employed. (58–61) An alkyne then coordinates in a side-on fashion to the metal hydrido species, which subsequently inserts into the metal–hydride bond. This is followed by reductive elimination to form the silicon-containing alkenyl products, along with the formation of an  $M^I$  species. (58) Depending on the ancillary ligands employed, facile cycling between  $M^I$  and  $M^{III}$  is often hindered, which may hamper the catalytic activity for such a reaction. (62) It was therefore necessary to consider alternative pathways and mechanisms in the case of highly active  $Cp^*MCl$  species ( $M = Rh, Ir$ ) to adequately describe pathways that catalytically active intermediates follow in order to account for their (high) activity. One such proposal was reported by Jiménez and Pérez-Torrente (56) and was used in order to propose a mechanism (Scheme 4).



**Scheme 4.** Proposed Catalytic Cycle for the Cp<sup>\*</sup>Rh-Catalyzed Hydrosilylation of Internal Alkynes

In this mechanism, the precatalysts (**1–4**) are activated by chlorido ligand substitution with H<sub>2</sub>SiPh<sub>2</sub> to provide the [Rh]-H species (**A**) and HSiPh<sub>2</sub>Cl. Hydride transfer occurs from the silyl ligand to the alkyl tether to form a formally bonded SiHPh<sub>2</sub> ligand as well as the corresponding free alkenyl tether (species **B**). A vacant coordination site in **B** is available for incoming alkyne coordination (species **C**). Insertion of the alkyne ligand into the Rh–Si bond forms the Rh vinylsilane adduct (species **D**). At this point isomerization from the β-(*E*) to the β-(*Z*) isomer is possible (not shown), as has been described in detail in the literature. (56,63) Hydrogen transfer from the free tether onto the vinylsilane fragment then occurs to form the β-(*E*) alkenyl organic product (dissociated) and re-forms the active catalyst species **A** via the coordination of another molecule of H<sub>2</sub>SiPh<sub>2</sub>. Confirmation of an agostic hydrogen interaction was observed in the <sup>1</sup>H NMR spectrum when **2** was reacted with H<sub>2</sub>SiPh<sub>2</sub> and diphenylacetylene in a 1:1:1 ratio (Figure S24 in the Supporting Information). A characteristic hydride doublet was observed at –11.25 ppm (d, *J*<sub>RhH</sub> = 37.3 Hz, 1H) due to hydrogen–rhodium coupling. For the N-bound congeners (**1b**, **2b**) the standard Chalk–Harrod mechanism may be applied (included in Scheme S1 in the Supporting Information).

### Biological Application

All complexes displayed a cytotoxicity of <30 μM (Table 3); however, at present it is unclear whether this effect is due to the inhibition of growth or induction of cell death processes.

Cytotoxicity was especially prevalent in the BT-20 triple-negative breast carcinoma (3.71–8.82  $\mu\text{M}$ ) and MCF-12A nontumorigenic mammary gland (4.30–12.32  $\mu\text{M}$ ) cell lines. Complex **4** tended to be more cytotoxic, especially in the BT-20 triple-negative breast carcinoma (3.71  $\mu\text{M}$ ), MCF-12A nontumorigenic mammary gland cell (4.30  $\mu\text{M}$ ), MDA-MB-231 triple-negative breast carcinoma (5.73  $\mu\text{M}$ ), and MCF-7/TAMR-1 tamoxifen-resistant subtype of the MCF-7 estrogen- and progesterone-positive luminal breast carcinoma cell lines (5.23  $\mu\text{M}$ ) in comparison to the rest of the complexes. Cancer selectivity indices (relative to MCF-12A) suggest that none of the complexes were ideally selective toward any specific cancerous cell line, with values varying between 0.30 and 1.40 (Table 4). Although a selectivity index  $\geq 3$  has been suggested as a potential indicator of good anticancer selectivity, others suggest  $\geq 10$ . (64) The complexes only displayed a greater preference toward the BT-20 cell line (1.11–1.40), although this would still be considered too low for selective action. The structure of the complexes affects the cytotoxicity and selectivity of the complex, (65,66) as can be seen from Table 4. In general, the complex containing more hydrophobic moieties (**3**, selectivity indices of 0.48–1.40) had better selectivity toward the selected cancer cell lines in comparison to the analogue with only a methyl group (**1**, selectivity indices of 0.36–1.16). It can also be seen that the NHC complex with a modified backbone (**4**, 3.71–12.74  $\mu\text{M}$ ) had a higher cytotoxicity in comparison to that of the analogue without backbone modification (**1**,  $\text{IC}_{50}$  values of 3.79–14.68  $\mu\text{M}$ ). All of the complexes thus appear to be nonselective in decreasing the cell density of the selected cell lines and will not serve as good candidates for anticancer assessment.

**Table 3.** Cytotoxicity of Complexes in the Various Cell Lines

complex	$\text{IC}_{50}$ ( $\mu\text{M}$ ) $\pm$ standard error of the mean (SEM)							
	A549	BT20	C2C12	HepG2	MCF-7	MCF-12A	MDA-MB-231	MCF-7/TAMR1
<b>1</b>	13.07 $\pm$ 1.04	3.79 $\pm$ 1.05	11.26 $\pm$ 1.1	8.58 $\pm$ 1.06	8.09 $\pm$ 1.04	4.40 $\pm$ 1.10	10.06 $\pm$ 1.03	14.68 $\pm$ 1.43
<b>2</b>	14.72 $\pm$ 1.05	3.98 $\pm$ 1.05	10.93 $\pm$ 1.36	12.22 $\pm$ 1.1	8.76 $\pm$ 1.03	4.40 $\pm$ 1.09	10.36 $\pm$ 1.04	12.15 $\pm$ 1.08
<b>3</b>	13.01 $\pm$ 1.04	8.82 $\pm$ 1.08	16.54 $\pm$ 1.03	24.08 $\pm$ 1.08	25.85 $\pm$ 1.01	12.32 $\pm$ 1.06	13.96 $\pm$ 1.05	17.48 $\pm$ 1.17
<b>4</b>	12.74 $\pm$ 1.04	3.71 $\pm$ 1.05	9.05 $\pm$ 1.04	12.66 $\pm$ 1.09	8.90 $\pm$ 1.03	4.30 $\pm$ 1.09	5.73 $\pm$ 1.14	5.23 $\pm$ 1.58

**Table 4.** Cancer Selectivity Indices of Complexes Relative to the MCF-12A Cell Line

complex	A549	BT20	C2C12	HepG2	MCF-7	MCF-12A	MDA-MB-231	MCF-7/TAMR1
<b>1</b>	0.34	1.16	0.39	0.51	0.54	1.00	0.44	0.30
<b>2</b>	0.30	1.11	0.40	0.36	0.50	1.00	0.42	0.36
<b>3</b>	0.95	1.40	0.74	0.51	0.48	1.00	0.88	0.70
<b>4</b>	0.34	1.16	0.48	0.34	0.48	1.00	0.75	0.82

## CONCLUSIONS

A series of novel self-isomerized–cyclometalated Rh-NHC complexes were synthesized, characterized, and successfully applied to the catalytic hydrosilylation of internal alkynes. The unique base-free intramolecular isomerization–cyclometalation process observed in the complexes was explored through NMR spectroscopy and SCXRD. The selectivity of rhodium cyclometalation was investigated by incorporation of a ligand system that included two possible linker systems (complex **3**), whereby the rhodium metal center showed an exclusive preference for cyclometalation via the alkenyl arm with the subsequent isomerization. These alkenyl systems proved to be interesting, undergoing cyclometalation/isomerization in addition to *N*-dealkylation, providing a range of unique bench-stable complexes.

For the hydrosilylation of the relatively inert internal alkynes these novel rhodium complexes showed notable catalytic activity as well as good functional group tolerance for the range of alkyne substrates studied. Even at a catalyst loading of 1 mol % complex **2** showed high activity and selectivity. The results therefore indicate that NHC complexes designed to contain carbon-based tethers are viable options to stabilize the metal center and provide a degree of hemilability (through self-isomerization) to increase the activity of the overall complex. The biological results showed some promise. Complex **4** was the most effective against the tested cancer cell lines. However, poor cancer selectivity (0.30–1.40) relative to the MCF-12A cell line was observed, suggesting that these compounds do not possess ideal antineoplastic characteristics in their present design. Future work will entail a modification of the design of the complexes to allow better selectivity against cancer cells by including biologically relevant moieties into the ligand design.

## EXPERIMENTAL SECTION

### General Considerations

All experiments were performed under an argon atmosphere using standard Schlenk techniques. Solvents were dried and distilled from appropriate drying agents prior to use. The imidazolium chloride salts (**L1–L5**) were synthesized according to previously reported methods. (25,26)  $[\text{Cp}^*\text{RhCl}_2]_2$  was synthesized via a previously reported method. (67) Other chemicals used were purchased from commercial suppliers and utilized without further purification.  $^1\text{H}$  (300/400 MHz) and  $^{13}\text{C}\{^1\text{H}\}$  (76 MHz) NMR spectra were recorded on either a Bruker Avance-400 or a Bruker Gemini 300 MHz spectrometer using  $\text{CDCl}_3$  unless otherwise stated. All measurements were performed at ambient temperature (298 K), unless otherwise stated. Chemical shifts were referenced to the internal residual solvent resonances. Electrospray mass spectra (ESI-MS) were recorded on a Micromass Quatro LC instrument. EA analyses were conducted at UKZN and the University of Pretoria using a ThermoScientific Flash2000 Elemental Analyzer.

### General Synthesis of Cyclometalated Rh-NHC Complexes

A suspension of the corresponding imidazolium chloride salt (1 mmol) in  $\text{CH}_2\text{Cl}_2$  (20 mL) containing  $\text{Ag}_2\text{O}$  (0.262 g, 1.2 mmol) was stirred at 30 °C for 1 h (12 h in the case of **4**) in the absence of light. The resulting mixture was filtered, after which time  $[\text{Cp}^*\text{RhCl}_2]_2$  (0.25 g, 0.4 mmol) was added and the resulting mixture was stirred at 30 °C for 24 h. The subsequent crude reaction mixture was filtered, concentrated *in vacuo*, and purified via silica gel column chromatography using gradient elution with  $\text{Et}_2\text{O}/\text{CHCl}_3/\text{acetone}$ . In some cases where byproducts were obtained, the byproducts were separated from  $[\text{Cp}^*\text{RhCl}_2]_2$  using aluminum oxide column chromatography with gradient elution ( $\text{CHCl}_3/\text{MeOH}$ ). A range of yellow to red solids were obtained.

Data for **1** are as follows. Yield: 35%.  $^1\text{H}$  NMR ( $\text{CDCl}_3$ ):  $\delta_{\text{H}}$  1.58 (s, 15H,  $\text{C}_{10}\text{H}_{15}$ ), 1.94 (s, 3H,  $\text{CCH}_3$ ), 1.95 (dd,  $J = 10.3, 3.5$  Hz, 1H, Rh-CH), 3.41 (d,  $J = 10.2$  Hz, 1H, Rh-CH), 4.03 (s, 3H,  $\text{NCH}_3$ ), 6.17 (s, 1H,  $\text{C}=\text{CH}$ ), 6.92 (d,  $J = 1.7$  Hz, 1H,  $\text{C}_{\text{imi}}\text{H}$ ), 6.96 (d,  $J = 1.7$  Hz, 1H,  $\text{C}_{\text{imi}}\text{H}$ ).  $^{13}\text{C}\{^1\text{H}\}$  NMR ( $\text{CDCl}_3$ ):  $\delta_{\text{C}}$  9.1 (s,  $\text{C}_{10}\text{H}_{15}$ ), 21.0 (d,  $J = 23.3$  Hz, Rh- $\text{C}_{\text{cyclometalated}}$ ), 23.2 (s,  $\text{CCH}_3$ ), 37.7 (s,  $\text{NCH}_3$ ), 95.3 (d,  $J_{\text{C-Rh}} = 5.2$  Hz,  $\text{C}_{\text{Cp}^*-\text{Rh}}$ ), 117.0 (s,  $\text{NCH}=\text{C}$ ), 118.4 (s,  $\text{C}_{\text{imi}}$ ), 123.1 (s,  $\text{C}_{\text{imi}}$ ), 138.7 (s,  $\text{CCH}_3$ ), 175.4 (d,  $J = 58.7$  Hz, Rh- $\text{C}_{\text{carbene}}$ ). HR-MS (ESI)  $m/z$  found (calcd): ( $\text{M}^+ - \text{Cl} - \text{CH}_3$ ) 359.0992 (359.0995) calcd for  $\text{C}_{17}\text{H}_{24}\text{N}_2\text{Rh}$ . Anal. Found (calcd) for  $[\text{C}_{18}\text{H}_{26}\text{ClN}_2\text{Rh}]$ : C, 52.49 (52.89); H, 6.49 (6.41); N, 6.49 (6.85).

Data for **2** are as follows. Yield: 50%.  $^1\text{H}$  NMR ( $\text{CDCl}_3$ ):  $\delta_{\text{H}}$  1.58 (s, 15H,  $\text{C}_{10}\text{H}_{15}$ ), 1.81 (s, 3H,  $\text{CCH}_3$ ), 1.95 (s, 3H,  $\text{CCH}_3$ ), 1.97–2.00 (m, 1H, Rh- $\text{CH}_2$ ), 3.39–3.43 (m, 1H, Rh- $\text{CH}_2$ ), 4.83 (d,  $J = 15.2$  Hz, 1H,  $\text{NCH}_2\text{C}$ ), 4.96 (s, 1H,  $\text{C}=\text{CH}_2$ ), 5.06 (s, 1H,  $\text{C}=\text{CH}_2$ ), 5.25 (d,  $J = 15.2$  Hz, 1H,  $\text{NCH}_2\text{C}$ ), 6.18 (s, 1H,  $\text{NCH}=\text{C}$ ), 6.95 (s, 1H,  $\text{C}_{\text{imi}}\text{H}$ ), 6.99 (s, 1H,  $\text{C}_{\text{imi}}\text{H}$ ).  $^{13}\text{C}\{^1\text{H}\}$  NMR ( $\text{CDCl}_3$ ):  $\delta_{\text{C}}$  9.2 (s,  $\text{C}_{10}\text{H}_{15}$ ), 20.4 (s,  $\text{CCH}_3$ ), 21.2 (d,  $J = 23.2$  Hz, Rh-Cyclometalated), 23.2 (s,  $\text{CCH}_3$ ), 56.5 (s,  $\text{C}=\text{CH}_2$ ), 95.4 (d,  $J_{\text{C-Rh}} = 5.2$  Hz,  $\text{C}_{\text{Cp}^*-\text{Rh}}$ ), 114.5 (s,  $\text{NCH}_2\text{C}$ ), 116.9 (s,  $\text{NCH}=\text{C}$ ), 118.3 (s,  $\text{NC}=\text{C}$ ), 121.4 (s,  $\text{NCN}$ ), 139.1 (s,  $\text{C}_{\text{imi}}$ ), 141.5 (s,  $\text{C}_{\text{imi}}$ ) 176.0 (d,  $J = 59.2$  Hz, Rh- $\text{C}_{\text{carbene}}$ ). HR-MS (ESI)  $m/z$  found (calcd): 414.1536 ( $\text{M}^+ - \text{Cl}$ ) (414.1542) calcd for  $\text{C}_{21}\text{H}_{31}\text{N}_2\text{Rh}$ . Anal. Found (calcd) for  $[\text{C}_{21}\text{H}_{30}\text{ClN}_2\text{Rh}]$ : C, 55.32 (55.70); H, 7.32 (7.57); N, 6.36 (6.19).

Data for **3** are as follows. Yield: 70%.  $^1\text{H}$  NMR ( $\text{CDCl}_3$ ): 1.63 (s, 15H,  $\text{C}_{10}\text{H}_{15}$ ), 1.99 (s, 3H,  $\text{CCH}_3$ ), 2.05 (ddd,  $J = 10.3, 3.6, 1.3$  Hz, 1H, Rh- $\text{CH}_2$ ), 3.49 (dt,  $J = 10.5, 3.2$  Hz, 1H, Rh- $\text{CH}_2$ ), 5.25 (d,  $J = 14.3$  Hz, 1H,  $\text{NCH}_2\text{Ph}$ ), 6.11 (d,  $J = 14.3$  Hz, 1H,  $\text{NCH}_2\text{Ph}$ ), 6.21 (s, 1H,  $\text{NCH}=\text{C}$ ), 6.73 (d,  $J = 2.0$  Hz, 1H,  $\text{C}_{\text{imi}}\text{H}$ ), 6.91 (d,  $J = 2.0$  Hz, 1H,  $\text{C}_{\text{imi}}\text{H}$ ), 7.34–7.42 (m, 4H, Ph), 7.51–7.53 (m, 1H, Ph).  $^{13}\text{C}\{^1\text{H}\}$  NMR ( $\text{CDCl}_3$ ):  $\delta_{\text{C}}$  9.3 (s,  $\text{C}_{10}\text{H}_{15}$ ), 21.3 (d,  $J = 21.35$  Hz, Rh-Cyclometalated), 23.2 (s,  $\text{CCH}_3$ ), 54.3 (s,  $\text{NCH}_2\text{Ph}$ ), 95.5 (d,  $J_{\text{C-Rh}} = 5.2$  Hz,  $\text{C}_{\text{Cp}^*-\text{Rh}}$ ), 116.9 (s,  $\text{C}=\text{C}(\text{CH}_2)\text{CH}_3$ ), 118.3 (s,  $\text{NCH}=\text{C}$ ), 121.4 (s, Ph), 128.2 (s, Ph), 128.8 (s, Ph), 129.3 (s, Ph), 136.2 (s,  $\text{C}_{\text{imi}}$ ), 139.1 (s,  $\text{C}_{\text{imi}}$ ), 175.9 (d,  $J_{\text{Rh-C}} = 58.8$  Hz,  $\text{C}_{\text{carbene}}$ ). HR-MS (ESI)  $m/z$  found (calcd): ( $\text{M}^+$ ) 485.1224 (485.1231) calcd for  $\text{C}_{24}\text{H}_{31}\text{ClN}_2\text{Rh}$ . Anal. Found (calcd) for  $[\text{C}_{24}\text{H}_{30}\text{ClN}_2\text{Rh}]$ : C, 59.62 (59.45); H, 6.40 (6.24); N, 5.74 (5.78).

Data for **4** are as follows. Yield: 40%.  $^1\text{H}$  NMR ( $\text{CDCl}_3$ ):  $\delta_{\text{H}}$  1.60 (s, 15H,  $\text{C}_{10}\text{H}_{15}$ ), 1.95 (s, 3H,  $\text{CCH}_3$ ), 1.99–2.03 (m, 1H, Rh- $\text{CH}_2$ ), 2.21 (s, 3H,  $\text{CCH}_3$ ), 3.44 (dd,  $J = 6.9, 3.3$  Hz, 1H, Rh-Cyclometalated), 3.95 (s, 3H,  $\text{NCH}_3$ ), 6.13 (s, 1H,  $\text{NCH}=\text{C}$ ), 6.69 (s, 1H,  $\text{C}_{\text{imi}}\text{H}$ ).  $^{13}\text{C}\{^1\text{H}\}$  NMR ( $\text{CDCl}_3$ ):  $\delta_{\text{C}}$  8.1 (s,  $\text{C}_{10}\text{H}_{15}$ ), 9.1 (s,  $\text{CCH}_3$ ), 20.2 (d,  $J = 23.3$  Hz, Rh- $\text{CH}_2$ ), 22.1 (s,  $\text{C}_{\text{imi}}-\text{CH}_3$ ), 33.8 (s,  $\text{N}-\text{CH}_3$ ), 94.2 (d,  $J_{\text{C-Rh}} = 5.2$  Hz,  $\text{C}_{\text{Cp}^*-\text{Rh}}$ ), 114.6 (s,  $\text{NCH}=\text{C}$ ), 115.9 (s,  $\text{CH}=\text{C}$ ), 129.9 (s,  $\text{C}_{\text{imi}}$ ), 136.8 (s,  $\text{C}_{\text{imi}}$ ) 173.6 (d,  $J = 58.7$  Hz, Rh- $\text{C}_{\text{carbene}}$ ). HR-MS (ESI)  $m/z$  found (calcd): ( $\text{M}^+ - \text{Cl}$ ) 387.1300 (387.1308) calcd for  $\text{C}_{19}\text{H}_{28}\text{N}_2\text{Rh}$ . Anal. Found (calcd) for  $[\text{C}_{19}\text{H}_{28}\text{ClN}_2\text{Rh}]$ : C, 53.86 (53.97); H, 6.82 (6.68); N, 6.42 (6.63).

Data for **1b** are as follows. Yield 45%.  $^1\text{H}$  NMR ( $\text{CDCl}_3$ ):  $\delta_{\text{H}}$  1.58 (s, 15H,  $\text{C}_{10}\text{H}_{15}$ ), 3.63 (s, 3H,  $\text{NCH}_3$ ), 6.88 (s, 1H,  $\text{C}_{\text{imi}}\text{H}$ ), 7.13 (s, 1H,  $\text{C}_{\text{imi}}\text{H}$ ), 7.86 (s, 1H,  $\text{NCHN}$ ).  $^{13}\text{C}\{^1\text{H}\}$  NMR ( $\text{CDCl}_3$ ):  $\delta_{\text{C}}$  9.0 (s,  $\text{C}_{10}\text{H}_{15}$ ), 34.6 (s,  $\text{NCH}_3$ ), 93.6 (d,  $J_{\text{C-Rh}} = 8.4$  Hz,  $\text{C}_{\text{Cp}^*-\text{Rh}}$ ), 121.5 (s,  $\text{C}_{\text{imi}}$ ), 130.2 (s,  $\text{C}_{\text{imi}}$ ), 139.5 (s,  $\text{NCHN}$ ). HR-MS (ESI)  $m/z$  found (calcd): ( $\text{M}^+ - \text{Cl}$ ) 355.0464 (355.0448) calcd for  $\text{C}_{14}\text{H}_{21}\text{ClN}_2\text{Rh}$ . Anal. Found (calcd) for  $[\text{C}_{14}\text{H}_{21}\text{Cl}_2\text{N}_2\text{Rh}]$ : C, 43.37 (42.99); H, 5.71 (5.41); N, 6.95 (7.16).

Data for **1bd** are as follows. Yield: 100%.  $^1\text{H}$  NMR ( $(\text{CD}_3)_2\text{CO}$ ):  $\delta_{\text{H}}$  1.63 (s, 15H,  $\text{C}_{10}\text{H}_{15}$ ), 1.76 (s, 15H,  $\text{C}_{10}\text{H}_{15}$ ), 3.85 (s, 6H,  $\text{NCH}_3$ ), 7.33 (d,  $J = 1.5$  Hz, 2H,  $\text{C}_{\text{imi}}\text{H}$ ), 7.34 (d,  $J = 1.5$  Hz, 2H,  $\text{C}_{\text{imi}}\text{H}$ ), 8.11 (s, 1H,  $\text{NCHN}$ ).  $^{13}\text{C}\{^1\text{H}\}$  NMR ( $(\text{CD}_3)_2\text{CO}$ ):  $\delta_{\text{C}}$  8.0 (s,  $\text{C}_{10}\text{H}_{15}$ ), 8.7 (s,  $\text{C}_{10}\text{H}_{15}$ ), n.o. (s,  $\text{NCH}_3$ ), 95.2 ( $\text{Cp}^*$ ), 122.5 (s,  $\text{C}_{\text{imi}}$ ), 129.0 (s,  $\text{C}_{\text{imi}}$ ), 140.2 (s,  $\text{NCHN}$ ). HR-MS (ESI)  $m/z$  found (calcd): ( $\text{M}^+ - 2\text{Cl}$ ) 710.1016 (710.0987) calcd for  $\text{C}_{28}\text{H}_{42}\text{Cl}_2\text{N}_4\text{Rh}_2$ . Anal. Found (calcd) for  $[\text{C}_{28}\text{H}_{42}\text{Cl}_2\text{N}_4\text{Rh}_2]$ : C, 47.48 (47.27); H, 5.58 (5.95); N, 7.49 (7.88).

Data for **2b** are as follows. Yield: 35%.  $^1\text{H}$  NMR ( $\text{CDCl}_3$ ):  $\delta_{\text{H}}$  1.61 (s, 15H,  $\text{C}_{10}\text{H}_{15}$ ), 1.68 (s, 3H,  $\text{CCH}_3$ ), 4.43 (s, 2H,  $\text{NCH}_2\text{C}$ ), 4.80 (s, 1H,  $\text{C}=\text{CH}_2$ ), 5.00 (s, 1H,  $\text{C}=\text{CH}_2$ ), 6.89 (s, 1H,  $\text{C}_{\text{imi}}\text{H}$ ), 7.26 (s, 1H,  $\text{C}_{\text{imi}}\text{H}$ ), 7.94 (s, 1H,  $\text{NCHN}$ ).  $^{13}\text{C}\{^1\text{H}\}$  NMR ( $\text{CDCl}_3$ ):  $\delta_{\text{C}}$  9.0 (s,  $\text{C}_{10}\text{H}_{15}$ ), 19.7 ( $\text{CCH}_3$ ), 54.1 (s,  $=\text{CH}_2$ ), 93.5 (d,  $J_{\text{C-Rh}} = 8.4$  Hz,  $\text{C}_{\text{Cp}^*-\text{Rh}}$ ), 114.9 (s,  $\text{N}-\text{CH}_2$ ), 120.4 ( $\text{C}_{\text{imi}}$ ), 130.4 (s,  $\text{C}_{\text{imi}}$ ), 139.4 (s,  $\text{CCH}_3$ ), 139.6 (s,  $\text{NCHN}$ ). HR-MS (ESI)  $m/z$  found (calcd):

( $M^+ - \text{CH}_2(=\text{CH}_2)\text{CH}_3$ ) 375.9975 (375.9980) calcd for  $\text{C}_{13}\text{H}_{19}\text{Cl}_2\text{N}_2\text{Rh}$ . Anal. Found (calcd) for  $[\text{C}_{17}\text{H}_{25}\text{Cl}_2\text{N}_2\text{Rh}]$ : C, 47.71 (47.35); H, 5.93 (6.09); N, 6.13 (6.50).

Data for **2bd** are as follows. Yield: 100%.  $^1\text{H}$  NMR ( $(\text{CD}_3)_2\text{CO}$ ):  $\delta_{\text{H}}$  1.42 (s, 6H,  $\text{CCH}_3$ ), 1.66, 1.67 (2s, 30H,  $\text{C}_{10}\text{H}_{15}$ ), 4.73 (s, 2H,  $\text{C}=\text{CH}_2$ ), 4.76 (s, 4H,  $\text{NCH}_2\text{C}$ ), 4.97 (s, 2H,  $\text{C}=\text{CH}_2$ ), 7.33 (t,  $J = 1.6$  Hz, 2H,  $\text{C}_{\text{imi}}\text{H}$ ), 7.39 (t,  $J = 1.3$  Hz, 2H,  $\text{C}_{\text{imi}}\text{H}$ ), 8.17 (s, 1H,  $\text{NCHN}$ ).  $^{13}\text{C}\{^1\text{H}\}$  NMR ( $\text{CDCl}_3$ ):  $\delta_{\text{C}}$  8.8 (s,  $\text{C}_{10}\text{H}_{15}$ ), 19.4 ( $\text{CCH}_3$ ), 54.0 (s,  $=\text{CH}_2$ ), 95.4 (d,  $J_{\text{C-Rh}} = 8.4$  Hz,  $\text{C}_{\text{Cp}^*-\text{Rh}}$ ), 114.8 (s,  $\text{N-CH}_2$ ), 120.8 ( $\text{C}_{\text{imi}}$ ), 130.0 (s,  $\text{C}_{\text{imi}}$ ), 139.2 (s,  $\text{CCH}_3$ ), 139.8 (s,  $\text{NCHN}$ ). HR-MS (ESI)  $m/z$  found (calcd): ( $M^+ - 2\text{Cl}$ ) 790.1523 (790.1523) calcd for  $\text{C}_{34}\text{H}_{50}\text{Cl}_2\text{N}_4\text{Rh}_2$ . Anal. Found (calcd) for  $[\text{C}_{34}\text{H}_{50}\text{Cl}_2\text{N}_4\text{Rh}_2]$ : C, 51.24 (51.59); H, 6.43 (6.37); N, 7.47 (7.08).

### Procedure for Hydrosilylation of Internal Alkynes

In an NMR tube containing diphenylacetylene (18 mg, 0.1 mmol), anisole as an internal standard (11  $\mu\text{L}$ , 0.1 mmol), and a rhodium complex (2 mg, 4 mol %) was placed diphenylsilane (10  $\mu\text{L}$ , 0.11 mmol) along with 1 mL of  $\text{C}_6\text{D}_6$ .  $^1\text{H}$  NMR spectroscopy was done at time = 0 h followed by placing the tightly sealed vessel in an oil bath at 80 °C for 1 h. A  $^1\text{H}$  NMR spectrum was taken shortly after the removal of the NMR tube from the oil bath. Conversions and isomer yields were determined from the integration of  $^1\text{H}$  NMR peaks relative to anisole as the internal standard, with the runs being performed in duplicate. TOF values were determined by using the conversion determined after the first 10 min of the reaction.

### X-ray Crystallography

A single-crystal diffraction experiment of complex **1** was performed using Quazar multilayer optics monochromated Mo  $K\alpha$  radiation ( $\lambda = 0.71069$  Å) on a Bruker D8 Venture kappa geometry diffractometer with dual  $\text{I}\mu\text{s}$  sources, a Photon 100 CMOS detector, and APEX III control software. (68) Data reduction was performed using SAINT+, (68) and the intensities were corrected for absorption using SADABS. (68) Single crystals of **L1**, **2**, **3**, **4**, **1b**, **1bd**, and **2bd** were analyzed on a Rigaku XtaLAB Synergy R diffractometer, with a rotating-anode X-ray source and a HyPix CCD detector. Data reduction and absorption were carried out using the CrysAlisPro (version 1.171.40.23a) software package. (69) All X-ray diffraction measurements were performed at 150(1) K, using an Oxford Cryogenics Cryostat. All structures were solved by direct methods with SHELXTS-2013 (70) and refined using the SHELXL-2013 (71) algorithm. All H atoms were placed in geometrically idealized positions and constrained to ride on their parent atoms. For data collection and refinement parameters, see the Tables S1–S3 in the Supporting Information. The X-ray crystallographic coordinates for all structures have been deposited at the Cambridge Crystallographic Data Centre (CCDC), with deposition numbers CCDC 2065431–2065437 and 2081484. The data can be obtained free of charge from The Cambridge Crystallographic Data Centre via [www.ccdc.cam.ac.uk/data\\_request/cif](http://www.ccdc.cam.ac.uk/data_request/cif).

### Biological Application

The cytotoxicity of the complexes was determined using the sulforhodamine B staining assay as described by Vichai and Kirtikara (72) with minor modifications to the volumes used. Several cell line types were used, with their respective concentrations and culturing methods being indicated in Table 5. All of the culture medium was supplemented with 1% penicillin/streptomycin and 10% fetal calf serum (FCS) as standard additives. Cell lines were



maintained in 75 cm<sup>2</sup> cell culture flasks with their respective medium in a humidified incubator with an environment of 37 °C and 5% carbon dioxide. Confluent flasks were washed with phosphate-buffered saline, after which cells were chemically detached using trypsinization. Cells were harvested using centrifugation (200g at 5 min) and diluted to the appropriate concentrations (10-fold of their seeding densities) in their respective media after counting using the trypan blue exclusion assay.

**Table 5.** Cell lines and Associated Culture Parameters Used for Cytotoxicity Assessment<sup>a</sup>

cell line	ATCC number	description	seeding density (cells/well)	culture medium
AS49	CCL-185	adenocarcinomic human alveolar basal epithelial cells	5000	advanced DMEM
BT-20	HTB-19	triple-negative breast carcinoma	5000	advanced DMEM
C2C12	CRL-1772	nontumorigenic myoblast cells	5000	advanced DMEM
HepG2	HB-8065	hepatocarcinoma	5000	advanced DMEM
MCF-7	HTB-22	estrogen- and progesterone-positive luminal breast carcinoma	5 000	advanced DMEM
MCF-7 Tam1	CRL-3435	tamoxifen-resistant subtype of MCF-7 cell line	5000	advanced DMEM, supplemented with 10 µg/mL human insulin and 1 µM 4-hydroxytamoxifen
MCF-12A	CRL-10782	nontumorigenic mammary gland cells	5000	A 1:1 mixture of DMEM and Ham's F12 medium, supplemented with 20 ng/mL human epidermal growth factor, 100 ng/mL cholera toxin, 0.01 mg/mL bovine insulin. and 500 ng/mL hydrocortisone
MDA-MB-231	HTB-26	triple-negative breast carcinoma	5000	advanced DMEM

<sup>a</sup>Abbreviations: ATCC, American Type Culture Collection; DMEM, Dulbecco's Modified Eagle Medium.

Cells (100 µL) were seeded into the wells of 96-well plates and allowed to attach overnight to the culture vessel. Cells were exposed to 100 µL of the medium (negative control), positive control (1% saponin), or samples (half-log dilutions of 200 µM) prepared in media supplemented with 10% FCS for 72 h. Blanks consisted of 200 µL pf 10% fetal calf serum supplemented medium. Exposed cells were fixed overnight with 50 µL of trichloroacetic acid (50%) at 4 °C. Fixed cells were washed three times using tap water and allowed to dry. Dried plates were stained with 100 µL of sulforhodamine B staining solution (0.057% in 1% acetic acid) for 30 min, after which they were washed three times with 150 µL of acetic acid (1%). Plates were allowed to dry after washing, and the bound dye was dissolved using 200 µL of Tris-base solution (10 mM, pH 10.5) for 60 min on a shaker. Plates were read spectrophotometrically using an ELX800 plate reader (Bio-Tek Instruments, Inc.) at 510 nm (reference wavelength 630 nm). Absorbance data were blank-excluded, and the percentage cell density relative to the negative control was calculated. Nonlinear regression was used to determine the half-maximum inhibitory concentration (IC<sub>50</sub>) using GraphPad Prism 5.0. Cancer selectivity indices of the complexes were expressed as the IC<sub>50</sub> value of the complex in the MCF-12A cell line expressed relative to the IC<sub>50</sub> value of the complex in the cancerous cell line.

## NOTES

The authors declare no competing financial interest.

## ACKNOWLEDGMENTS

This work was financially supported by the National Research Foundation of South Africa (ML Grant No. 120840, FPM Grant No. 117995) and the University of Pretoria.

## REFERENCES

- 1** Gardiner, M. G.; Ho, C. C. Recent advances in bidentate bis(N-heterocyclic carbene) transition metal complexes and their applications in metal-mediated reactions. *Coord. Chem. Rev.* **2018**, *375*, 373– 388, DOI: 10.1016/j.ccr.2018.02.003
- 2** Gil, W.; Trzeciak, A. M. N-Heterocyclic carbene–rhodium complexes as catalysts for hydroformylation and related reactions. *Coord. Chem. Rev.* **2011**, *255* (3–4), 473– 483, DOI: 10.1016/j.ccr.2010.11.005
- 3** Han, Y.-F.; Jin, G.-X. Cyclometalated [Cp\*M(C $\wedge$ X)] (M= Ir, Rh; X= N, C, O, P) complexes. *Chem. Soc. Rev.* **2014**, *43* (8), 2799– 2823, DOI: 10.1039/C3CS60343A
- 4** Poyatos, M.; Mata, J. A.; Peris, E. Complexes with Poly(N-heterocyclic carbene) Ligands: Structural Features and Catalytic Applications. *Chem. Rev.* **2009**, *109*, 3677– 3707, DOI: 10.1021/cr800501s
- 5** van Vuuren, E.; Malan, F. P.; Landman, M. Multidentate NHC complexes of Group IX metals featuring carbon-based tethers: synthesis and applications. *Coord. Chem. Rev.* **2021**, *430*, 213731, DOI: 10.1016/j.ccr.2020.213731
- 6** Colby, D. A.; Tsai, A. S.; Bergman, R. G.; Ellman, J. A. Rhodium catalyzed chelation-assisted C–H bond functionalization reactions. *Acc. Chem. Res.* **2012**, *45* (6), 814– 825, DOI: 10.1021/ar200190g
- 7** Song, G.; Li, X. Substrate activation strategies in rhodium(III)-catalyzed selective functionalization of arenes. *Acc. Chem. Res.* **2015**, *48* (4), 1007– 1020, DOI: 10.1021/acs.accounts.5b00077
- 8** Piou, T.; Rovis, T. Electronic and steric tuning of a prototypical piano stool complex: Rh(III) catalysis for C–H functionalization. *Acc. Chem. Res.* **2018**, *51* (1), 170– 180, DOI: 10.1021/acs.accounts.7b00444
- 9** Ghorai, D.; Dutta, C.; Choudhury, J. Switching of “Rollover Pathway” in Rhodium(III)-Catalyzed C–H Activation of Chelating Molecules. *ACS Catal.* **2016**, *6* (2), 709– 713, DOI: 10.1021/acscatal.5b02540
- 10** Thenarukandiyil, R.; Thrikkykkal, H.; Choudhury, J. Rhodium(III)-Catalyzed Nonaromatic sp<sup>2</sup> C–H Activation/Annulation Using NHC as a Directing and Functionalizable Group. *Organometallics* **2016**, *35*, 3007– 3013, DOI: 10.1021/acs.organomet.6b00530
- 11** Ge, Q.; Li, B.; Song, H.; Wang, B. Rhodium(III)-catalyzed cascade oxidative annulation reactions of aryl imidazolium salts with alkynes involving multiple C–H bond activation. *Org. Biomol. Chem.* **2015**, *13* (28), 7695– 7710, DOI: 10.1039/C5OB00823A
- 12** Tan, K. L.; Bergman, R. G.; Ellman, J. A. Intermediacy of an N-Heterocyclic Carbene Complex in the Catalytic C–H Activation of a Substituted Benzimidazole. *J. Am. Chem. Soc.* **2002**, *124* (13), 3202– 3203, DOI: 10.1021/ja017351d

- 13** Ghorai, D.; Choudhury, J. Exploring a unique reactivity of N-heterocyclic carbenes (NHC) in rhodium(III)-catalyzed intermolecular C–H activation/annulation. *Chem. Commun.* **2014**, *50*, 15159– 15162, DOI: 10.1039/C4CC07170K
- 14** Tian, Y.; Jürgens, E.; Kunz, D. Regio- and chemoselective rearrangement of terminal epoxides into methyl alkyl and aryl ketones. *Chem. Commun.* **2018**, *54*, 11340– 11343, DOI: 10.1039/C8CC06503A
- 15** Downing, S. P.; Pogorzelec, P. J.; Danopoulos, A. A.; Cole-Hamilton, D. J. Indenyl- and Fluorenyl-Functionalized N-Heterocyclic Carbene Complexes of Rhodium and Iridium- Synthetic, Structural and Catalytic Studies. *Eur. J. Inorg. Chem.* **2009**, *2009*, 1816– 1824, DOI: 10.1002/ejic.200801162
- 16** Debono, N.; Daran, J.-C.; Poli, R.; Labande, A. A rhodium(I) dicarbonyl complex with a redox-active ferrocenyl phosphine-NHC ligand: Enhanced reactivity of the metal centre through ferrocene oxidation. *Polyhedron* **2015**, *86*, 57– 63, DOI: 10.1016/j.poly.2014.04.050
- 17** Böhmer, M.; Guisado-Barrios, G.; Kampert, F.; Roelfes, F.; Tan, T. T. Y.; Peris, E.; Hahn, F. E. Synthesis and Catalytic Applications of Heterobimetallic Carbene Complexes Obtained via Sequential Metalation of Two Bisazolium Salts. *Organometallics* **2019**, *38* (9), 2120– 2131, DOI: 10.1021/acs.organomet.9b00120
- 18** Bauer, E. B.; Andavan, G. S.; Hollis, T. K.; Rubio, R. J.; Cho, J.; Kuchenbeiser, G. R.; Helgert, T. R.; Letko, C. S.; Tham, F. S. Air-and Water-Stable Catalysts for Hydroamination/Cyclization. Synthesis and Application of CCC–NHC Pincer Complexes of Rh and Ir. *Org. Lett.* **2008**, *10* (6), 1175– 1178, DOI: 10.1021/ol8000766
- 19** Huckaba, A. J.; Hollis, T. K.; Reilly, S. W. Homobimetallic Rhodium NHC Complexes as Versatile Catalysts for Hydrosilylation of a Multitude of Substrates in the Presence of Ambient Air. *Organometallics* **2013**, *32* (21), 6248– 6256, DOI: 10.1021/om400452q
- 20** Zhao, Q.; Meng, G.; Nolan, S. P.; Szostak, M. N-heterocyclic carbene complexes in C–H activation reactions. *Chem. Rev.* **2020**, *120* (4), 1981– 2048, DOI: 10.1021/acs.chemrev.9b00634
- 21** Li, J.; Peng, J.; Bai, Y.; Lai, G.; Li, X. Synthesis of rhodium N-heterocyclic carbene complexes and their catalytic activity in the hydrosilylation of alkenes in ionic liquid medium. *J. Organomet. Chem.* **2011**, *696*, 2116– 2121, DOI: 10.1016/j.jorganchem.2010.11.017
- 22** Andavan, G. T. S.; Bauer, E. B.; Letko, C. S.; Hollis, T. K.; Tham, F. S. Synthesis and characterization of a free phenylene bis(N-heterocyclic carbene) and its di-Rh complex: Catalytic activity of the di-Rh and CCC–NHC Rh pincer complexes in intermolecular hydrosilylation of alkynes. *J. Organomet. Chem.* **2005**, *690*, 5938– 5947, DOI: 10.1016/j.jorganchem.2005.07.088
- 23** van den Broeke, J.; Winter, F.; Deelman, B.-J.; van Koten, G. A highly fluororous room-temperature ionic liquid exhibiting fluororous biphasic behavior and its use in catalyst recycling. *Org. Lett.* **2002**, *4* (22), 3851– 3854, DOI: 10.1021/ol026700l

- 24** Li, J.; Peng, J.; Bai, Y.; Zhang, G.; Lai, G.; Li, X. Phosphines with 2-imidazolium ligands enhance the catalytic activity and selectivity of rhodium complexes for hydrosilylation reactions. *J. Organomet. Chem.* **2010**, *695* (3), 431–436, DOI: 10.1016/j.jorganchem.2009.10.029
- 25** Malan, F. P.; Singleton, E.; Van Rooyen, P. H.; Albrecht, M.; Landman, M. Synthesis, Stability, and (De)hydrogenation Catalysis by Normal and Abnormal Alkene- and Picolyl-Tethered NHC Ruthenium Complexes. *Organometallics* **2019**, *38* (13), 2624–2635, DOI: 10.1021/acs.organomet.9b00178
- 26** Malan, F. P.; Singleton, E.; van Rooyen, P. H.; Landman, M. Tandem transfer hydrogenation–epoxidation of ketone substrates catalysed by alkene-tethered Ru(II)-NHC complexes. *New J. Chem.* **2019**, *43* (22), 8472–8481, DOI: 10.1039/C9NJ01220F
- 27** Braunstein, P.; Naud, F. Hemilability of Hybrid Ligands and the Coordination Chemistry of Oxazoline-Based Systems. *Angew. Chem., Int. Ed.* **2001**, *40* (4), 680–699, DOI: 10.1002/1521-3773(20010216)40:4<680::AID-ANIE6800>3.0.CO;2-0
- 28** Oertel, A. M.; Freudenreich, J.; Gein, J.; Ritleng, V.; Veiros, L. F.; Chetcuti, M. J. Intramolecular Nitrile C–H Bond Activation in Nickel NHC Complexes: A Route to New Nickelacycles. *Organometallics* **2011**, *30* (12), 3400–3411, DOI: 10.1021/om200246k
- 29** Canac, Y.; Duhayon, C.; Chauvin, R. A Diaminocarbene–Phosphonium Ylide: Direct Access to C,C Chelating Ligands. *Angew. Chem., Int. Ed.* **2007**, *46* (33), 6313–6315, DOI: 10.1002/anie.200701490
- 30** Canac, Y.; Lepetit, C.; Abdalilah, M.; Duhayon, C.; Chauvin, R. Diaminocarbene and Phosphonium Ylide Ligands: A Systematic Comparison of their Donor Character. *J. Am. Chem. Soc.* **2008**, *130* (26), 8406–8413, DOI: 10.1021/ja801159v
- 31** Chianese, A. R.; Zeglis, B. M.; Crabtree, R. H. Unexpected oxidative C–C cleavage in the metallation of 2-substituted imidazolium salts to give N-heterocyclic carbene complexes. *Chem. Commun.* **2004**, (19), 2176–2177, DOI: 10.1039/B409672J
- 32** Voutchkova, A. M.; Feliz, M.; Clot, E.; Eisenstein, O.; Crabtree, R. H. Imidazolium Carboxylates as Versatile and Selective N-Heterocyclic Carbene Transfer Agents: Synthesis, Mechanism, and Applications. *J. Am. Chem. Soc.* **2007**, *129* (42), 12834–12846, DOI: 10.1021/ja0742885
- 33** Ling, Z.; Yun, L.; Liu, L.; Wu, B.; Fu, X. Aerobic oxidative N-dealkylation of tertiary amines in aqueous solution catalyzed by rhodium porphyrins. *Chem. Commun.* **2013**, *49* (39), 4214–4216, DOI: 10.1039/C2CC37263K
- 34** Kim, J. H.; Grebies, S.; Boultadakis-Arapinis, M.; Daniliuc, C.; Glorius, F. Rh(I)/NHC\*-Catalyzed Site- and Enantioselective Functionalization of C(sp<sup>3</sup>)-H Bonds Toward Chiral Triarylmethanes. *ACS Catal.* **2016**, *6* (11), 7652–7656, DOI: 10.1021/acscatal.6b02392
- 35** Zenkina, O. V.; Keske, E. C.; Wang, R.; Crudden, C. M. Double Single-Crystal-to-Single-Crystal Transformation and Small-Molecule Activation in Rhodium NHC Complexes. *Angew. Chem., Int. Ed.* **2011**, *50* (35), 8100–8104, DOI: 10.1002/anie.201103316

- 36** Dorta, R.; Stevens, E. D.; Nolan, S. P. Double C–H Activation in a Rh–NHC Complex Leading to the Isolation of a 14-Electron Rh(III) Complex. *J. Am. Chem. Soc.* **2004**, *126* (16), 5054– 5055, DOI: 10.1021/ja049545+
- 37** Scott, N. M.; Dorta, R.; Stevens, E. D.; Correa, A.; Cavallo, L.; Nolan, S. P. Interaction of a Bulky N-Heterocyclic Carbene Ligand with Rh(I) and Ir(I). Double C-H Activation and Isolation of Bare 14-Electron Rh(III) and Ir(III) Complexes. *J. Am. Chem. Soc.* **2005**, *127* (10), 3516– 3526, DOI: 10.1021/ja043249f
- 38** Karataş, M. O.; Di Giuseppe, A.; Passarelli, V.; Alıcı, B.; Pérez-Torrente, J. J.; Oro, L. A.; Özdemir, I.; Castarlenas, R. Pentacoordinated rhodium(I) complexes supported by coumarin-functionalized N-heterocyclic carbene ligands. *Organometallics* **2018**, *37* (2), 191– 202, DOI: 10.1021/acs.organomet.7b00750
- 39** Drover, M. W.; Bowes, E. G.; Love, J. A.; Schafer, L. L. Accessing  $\delta$ -B–H Coordinated Complexes of Rh(I) and Ir(I) Using Mono- and Dihydroboranes: Cooperative Stabilization by a Phosphoramidate Coligand. *Organometallics* **2017**, *36* (2), 331– 341, DOI: 10.1021/acs.organomet.6b00784
- 40** Wiedemann, S. H.; Lewis, J. C.; Ellman, J. A.; Bergman, R. G. Experimental and Computational Studies on the Mechanism of N-Heterocycle C–H Activation by Rh(I). *J. Am. Chem. Soc.* **2006**, *128* (7), 2452– 2462, DOI: 10.1021/ja0576684
- 41** Ito, J.-I.; Sugino, K.; Matsushima, S.; Sakaguchi, H.; Iwata, H.; Ishihara, T.; Nishiyama, H. Synthesis of NHC-Oxazoline Pincer Complexes of Rh and Ru and Their Catalytic Activity for Hydrogenation and Conjugate Reduction. *Organometallics* **2016**, *35*, 1885– 1894, DOI: 10.1021/acs.organomet.6b00239
- 42** Cross, W. B.; Daly, C. G.; Boutadla, Y.; Singh, K. Variable coordination of amine functionalised N-heterocyclic carbene ligands to Ru, Rh and Ir: C–H and N–H activation and catalytic transfer hydrogenation. *Dalton Trans.* **2011**, *40*, 9722– 9730, DOI: 10.1039/c1dt10753d
- 43** Segarra, C.; Mas-Marzá, E.; Benítez, M.; Mata, J. A.; Peris, E. Unconventional Reactivity of Imidazolylidene Pyridylidene Ligands in Iridium(III) and Rhodium(III) Complexes. *Angew. Chem., Int. Ed.* **2012**, *51*, 10841– 10845, DOI: 10.1002/anie.201206175
- 44** Aznarez, F.; Sanz Miguel, P. J.; Tan, T. T. Y.; Hahn, F. E. Preparation of Rhodium(III) Di-NHC Chelate Complexes Featuring Two Different NHC Donors via a Mild NaOAc-Assisted C–H Activation. *Organometallics* **2016**, *35* (3), 410– 419, DOI: 10.1021/acs.organomet.5b00993
- 45** Albrecht, M. C4-bound imidazolylidenes: from curiosities to high-impact carbene ligands. *Chem. Commun.* **2008**, *31*, 3601– 3610, DOI: 10.1039/b806924g
- 46** Crabtree, R. H. Abnormal, mesoionic and remote N-heterocyclic carbene complexes. *Coord. Chem. Rev.* **2013**, *257* (3–4), 755– 766, DOI: 10.1016/j.ccr.2012.09.006

- 47** Liu, B.; De Brabander, J. K. Metal-catalyzed regioselective oxy-functionalization of internal alkynes: an entry into ketones, acetals, and spiroketals. *Org. Lett.* **2006**, *8* (21), 4907–4910, DOI: 10.1021/ol0619819
- 48** Trost, B. M.; Ball, Z. T. Addition of Metalloid Hydrides to Alkynes: Hydrometallation with Boron, Silicon, and Tin. *Synthesis* **2005**, *2005* (06), 853–887, DOI: 10.1055/s-2005-861874
- 49** Roy, A. K.; West, R.; Hill, A. F.; Fink, M. J. A Review of Recent Progress in Catalyzed Homogeneous Hydrosilylation (Hydrosilylation). *Adv. Organomet. Chem.* **2007**, *55*, 1–59, DOI: 10.1016/S0065-3055(07)55001-X
- 50** Morales-Ceron, J. P.; Lara, P.; López-Serrano, J.; Santos, L. L.; Salazar, V.; Alvarez, E.; Suárez, A. Rhodium(I) Complexes with Ligands Based on N-Heterocyclic Carbene and Hemilabile Pyridine Donors as Highly E Stereoselective Alkyne Hydrosilylation Catalysts. *Organometallics* **2017**, *36* (13), 2460–2469, DOI: 10.1021/acs.organomet.7b00361
- 51** Mas-Marzá, E.; Sanaú, M.; Peris, E. Coordination versatility of pyridine-functionalized N-heterocyclic carbenes: A detailed study of the different activation procedures. characterization of new Rh and Ir compounds and study of their catalytic activity. *Inorg. Chem.* **2005**, *44* (26), 9961–9967, DOI: 10.1021/ic051272b
- 52** Jiménez, M. V.; Pérez-Torrente, J. J.; Bartolomé, M. I.; Gierz, V.; Lahoz, F. J.; Oro, L. A. Rhodium(I) complexes with hemilabile N-heterocyclic carbenes: Efficient alkyne hydrosilylation catalysts. *Organometallics* **2008**, *27* (2), 224–234, DOI: 10.1021/om700728a
- 53** Cassani, M. C.; Brucka, M. A.; Femoni, C.; Mancinelli, M.; Mazzanti, A.; Mazzoni, R.; Solinas, G. N-Heterocyclic carbene rhodium(I) complexes containing an axis of chirality: dynamics and catalysis. *New J. Chem.* **2014**, *38* (4), 1768–1779, DOI: 10.1039/C3NJ01620J
- 54** Wang, Q.; Tinnermann, H.; Tan, S.; Young, R. D. Late-Stage Generation of Bidentate  $\eta^3$ -Benzophosphorine–Phosphino Ligands from a Rhodium PC<sub>carbene</sub>P Pincer Complex and Their Use in the Catalytic Hydrosilylation of Alkynes. *Organometallics* **2019**, *38* (19), 3512–3520, DOI: 10.1021/acs.organomet.9b00314
- 55** Sánchez-Page, B.; Jiménez, M. V.; Pérez-Torrente, J. J.; Passarelli, V.; Blasco, J.; Subias, G.; Granda, M.; Álvarez, P. Hybrid Catalysts Comprised of Graphene Modified with Rhodium-Based N-Heterocyclic Carbenes for Alkyne Hydrosilylation. *ACS Appl. Nano Mater.* **2020**, *3* (2), 1640–1655, DOI: 10.1021/acsanm.9b02398
- 56** Sánchez-Page, B.; Munarriz, J.; Jiménez, M. V.; Pérez-Torrente, J. J.; Blasco, J.; Subias, G.; Passarelli, V.; Álvarez, P.  $\beta$ -(Z) Selectivity Control by Cyclometalated Rhodium(III)–Triazolylidene Homogeneous and Heterogeneous Terminal Alkyne Hydrosilylation Catalysts. *ACS Catal.* **2020**, *10* (22), 13334–13351, DOI: 10.1021/acscatal.0c03295
- 57** Azpeitia, S.; Garralda, M. A.; Huertos, M. A. Rhodium(III) Catalyzed Solvent-Free Tandem Isomerization–Hydrosilylation From Internal Alkenes to Linear Silanes. *ChemCatChem.* **2017**, *9* (11), 1901–1905, DOI: 10.1002/cctc.201700222



- 58** Vicent, C.; Viciano, M.; Mas-Marzá, E.; Sanaú, M.; Peris, E. Electrospray ionization mass spectrometry studies on the mechanism of hydrosilylation of terminal alkynes using an N-heterocyclic carbene complex of iridium, allow detection/characterization of all reaction intermediates. *Organometallics* **2006**, *25* (15), 3713– 3720, DOI: 10.1021/om0602308
- 59** Jiménez, M. V.; Pérez-Torrente, J. J.; Bartolomé, M. I.; Gierz, V.; Lahoz, F. J.; Oro, L. A. Rhodium (I) complexes with hemilabile N-heterocyclic carbenes: Efficient alkyne hydrosilylation catalysts. *Organometallics* **2008**, *27* (2), 224– 234, DOI: 10.1021/om700728a
- 60** Cassani, M. C.; Brucka, M. A.; Femoni, C.; Mancinelli, M.; Mazzanti, A.; Mazzoni, R.; Solinas, G. N-Heterocyclic carbene rhodium (I) complexes containing an axis of chirality: dynamics and catalysis. *New J. Chem.* **2014**, *38* (4), 1768– 1779, DOI: 10.1039/C3NJ01620J
- 61** Corre, Y.; Werlé, C.; Brelot-Karmazin, L.; Djukic, J.-P.; Agbossou-Niedercorn, F.; Michon, C. Regioselective hydrosilylation of terminal alkynes using pentamethylcyclopentadienyl iridium(III) metallacycle catalysts. *J. Mol. Catal.* **2016**, *423*, 256– 263, DOI: 10.1016/j.molcata.2016.07.014
- 62** Morales-Ceron, J. P.; Lara, P.; López-Serrano, J.; Santos, L. L.; Salazar, V.; Alvarez, E.; Suárez, A. Rhodium (I) Complexes with Ligands Based on N-Heterocyclic Carbene and Hemilabile Pyridine Donors as Highly E Stereoselective Alkyne Hydrosilylation Catalysts. *Organometallics* **2017**, *36* (13), 2460– 2469, DOI: 10.1021/acs.organomet.7b00361
- 63** Roemer, M.; Gonçalves, V. R.; Keaveney, S. T.; Pernik, I.; Lian, J.; Downes, J.; Gooding, J. J.; Messerle, B. A. Carbon supported hybrid catalysts for controlled product selectivity in the hydrosilylation of alkynes. *Catal. Sci. Technol.* **2021**, *11* (5), 1888– 1898, DOI: 10.1039/D0CY02136A
- 64** Indrayanto, G.; Putra, G. S.; Suhud, F., Validation of in-vitro bioassay methods: Application in herbal drug research. In *Profiles of Drug Substances, Excipients, and Related Methodology*; Al-Majed, A. A., Ed.; Academic Press: 2021; Vol. 46, pp 273– 307.
- 65** Liu, Z.; Sadler, P. J. Organoiridium Complexes: Anticancer Agents and Catalysts. *Acc. Chem. Res.* **2014**, *47* (4), 1174– 1185, DOI: 10.1021/ar400266c
- 66** Liu, Z.; Habtemariam, A.; Pizarro, A. M.; Fletcher, S. A.; Kisova, A.; Vrana, O.; Salassa, L.; Buijninx, P. C. A.; Clarkson, G. J.; Brabec, V.; Sadler, P. J. Organometallic Half-Sandwich Iridium Anticancer Complexes. *J. Med. Chem.* **2011**, *54* (8), 3011– 3026, DOI: 10.1021/jm2000932
- 67** White, C.; Yates, A.; Maitlis, P. M.; Heinekey, D. M. ( $\eta^5$ -Pentamethylcyclopentadienyl) Rhodium and Iridium Compounds. *Inorg. Synth.* **2007**, 228– 234, DOI: 10.1002/9780470132609.ch53
- 68** SAINT; Bruker AXS Inc.: 2007.
- 69** CrysAlis PRO Software System; Rigaku Corporation: 2018.

**70** Sheldrick, G. M. SHELXT—Integrated space-group and crystal-structure determination. *Acta Crystallogr. A* **2015**, *71* (1), 3– 8, DOI: 10.1107/S2053273314026370

**71** Sheldrick, G. M. Crystal structure refinement with SHELXL. *Acta Crystallogr. C* **2015**, *71* (1), 3– 8, DOI: 10.1107/S2053229614024218

**72** Vichai, V.; Kirtikara, K. Sulforhodamine B colorimetric assay for cytotoxicity screening. *Nat. Protoc.* **2006**, *1* (3), 1112, DOI: 10.1038/nprot.2006.179